

**ATTACHMENT 5**

**Metallurgical Evaluations of a 'Boat' Sample from the #68 CRDM Penetration  
on Byron Unit 2**

**Exelon PowerLabs®, LLC.**  
Technical Services West  
36400 S. Essex Road  
Wilmington, IL 60481-9500

www.exelonpowerlabs.com  
815-458-7640  
815-458-7851 fax

**EXELON POWERLABS PROJECT BYR-48053**

**METALLURGICAL EVALUATIONS OF A 'BOAT' SAMPLE  
FROM THE #68 CRDM PENETRATION  
ON BYRON UNIT 2**

**REPORT DATE: MAY 23, 2007**

Reported by: Jim Chynoweth  
Senior Metallurgical Engineer  
Exelon PowerLabs West

Approved by: Jean Smith  
Corporate Engineering-Asset Management  
Exelon Nuclear

Concurrence: Jai Brihmadesan  
Technical Consultant to Exelon

## Executive Summary

In accordance with NRC Order EA-03-009 requirements, internal ultrasonic inspections were performed on the Byron Unit 2 reactor vessel head penetrations during the B2R13 outage. The inspections identified a 0.52" long x 0.326" deep axial indication near the J-groove weld in one of the 79 penetrations (i.e., #68 CRDM tube). A subsequent dye penetrant examination identified one axial and one rounded indication on the surface of #68 penetration J-groove weld approximately 16.5 degrees from the downhill azimuth.

A 'boat' sample was removed from the #68 penetration to determine the cause of the indications. The sample contained a portion of the axial indication but did not capture the rounded surface indication. The boat sample excavation also uncovered a sub-surface linear defect that intersected the axial indication. The sub-surface defect was partially captured by the boat sample.

The laboratory evaluations identified the axial indication as a combination of primary water stress corrosion cracking (PWSCC) and welding defects (i.e., lack of fusion and hot cracking). The sub-surface defect was identified as lack of fusion between the outer diameter (OD) of the tube and the J-groove weld. Within the boat sample, the cracking characteristics indicated the PWSCC initiated at a sub-surface location on the tube OD, propagated in an axial/radial direction into the tube, and propagated toward the wetted surface of the J-groove weld fillet leg.

The presence of PWSCC at this time is unexpected, since Byron Unit 2 is categorized as a low susceptibility plant per the methodology of NRC Order EA-03-009. The premature initiation is attributed to wetting of the tube OD surface at the sub-surface lack of fusion defect, which created a conducive crevice corrosion environment that allowed for PWSCC to initiate in the high stress region of the J-groove weld. The surface connected path for the lack of fusion defect was not contained in the boat sample but is attributed to the rounded surface indication that was not captured by the boat sample.

## 1.0 Background

In accordance with Nuclear Regulatory Commission (NRC) Order EA-03-009, ultrasonic inspections were performed on the inside of the Byron Unit 2 reactor head control rod drive mechanism (CRDM) tube penetrations during the B2R13 refueling outage. The inspections identified a 0.52" long x 0.326" deep axial indication in the #68 CRDM tube, near the J-groove weld (Figure 1). No indications were detected in the other 78 penetrations. The #68 penetration is a periphery tube and the maximum ultrasonic reflector was located 16.5° counter clockwise from the zero reference.

A dye penetrant (PT) examination was performed on the surface of the #68 penetration weld zone and the result is shown in Figure 2. The PT exam identified a 0.150" axial linear indication at the approximate orientation of the maximum ultrasonic reflector. In addition, a 0.050" diameter rounded indication was detected on the J-groove weld.

To evaluate the indications, a 'boat' sample was removed from the #68 tube and the J-groove weld by electrode discharge machining (EDM). However, the removed sample did not capture the rounded surface indication or the deepest portion of the axial indication (Figure 3). In addition, the excavation uncovered an angled, sub-surface defect that was connected to the axial indication. The remaining indications were left in the excavation and repaired in accordance with the Westinghouse embedded flaw weld overlay process.

This report documents the laboratory metallurgical evaluations that were performed on the removed boat sample. The primary objective was to determine the nature and cause of the indications in the boat sample.

## 2.0 Results and Conclusions

The boat sample contained a 0.032" long portion of the angled, sub-surface defect that was uncovered by the boat sample excavation. The defect was caused by lack of fusion between the next to last weld pass and the tube surface. The metallurgical sections identified several incipient cracks that had initiated from the sides of the lack of fusion crevice. Based on the field dye penetrant results, the lack of fusion defect was connected to the axial indication; although, this connection was not observed within the boat sample material.

The surface connected portion of the axial indication measured 0.18" long and was located in the fillet leg of the J-groove weld that was adjacent to the wrought tube. Within the weld, the axial indication exhibited multiple defect/crack morphologies that were characterized as lack of fusion between weld passes, welding hot cracks, primary water stress corrosion cracking (PWSCC), and local regions of ductile tearing between crack ligaments. The general direction of crack propagation was toward the wetted surface of the weld, which indicates the PWSCC cracking did not initiate from the wetted surface of the boat sample.

In the wrought tube material, the axial indication exhibited branched, intergranular features that were typical of PWSCC.

The tube/weld microstructures and chemistries were consistent with the specified materials (i.e., mill annealed Inconel 600 tube and Inconel 182 weld). Based on the presence of random intragranular carbides and partially decorated grain boundaries, the tube material had a relatively high susceptibility to PWSCC which is typical for mill annealed tubing produced during the 1970's.

The tube microhardness measurements ranged from equivalent values of 82.0 to 88.1 Rockwell B scale, which indicates there was not a high degree of cold working.

The weld surface exhibited heavy grinding that resulted in a 0.0007" thick cold worked layer and grinding laps. The microhardness measurements for the cold worked layer measured up to 25.3 Rockwell C scale. There was no evidence of crack initiation from the cold worked layer or the grinding laps.

Since Byron Unit 2 is categorized as a low susceptibility plant per NRC Order EA-03-009, the detection of PWSCC at this time is unexpected. The premature cracking and the detection of cracking in only one of 79 Byron Unit 2 nozzles suggests that an atypical condition was present with the #68 CRDM penetration. This conclusion is supported by the lack of detected cracking by the ultrasonic inspections of other Heat 80054 tube penetrations at Exelon plants (i.e., 28 additional tubes).

Based on the laboratory evaluations, the PWSCC cracking is attributed to the detected welding defects, a susceptible tube material microstructure, the existence of a tight crevice condition created by the welding defects, and the presence of high hoop stresses on the outer diameter of the tube at this location. The following is considered the most probable scenario for the PWSCC cracking.

- The original four layer welding process generated a sub-surface lack of fusion defect that was not detected by the fabrication surface non-destructive examination (NDE). The lack of fusion defect corresponds to the angled, sub-surface defect that was uncovered by the boat sample excavation and was partially captured in the boat sample.
- The fabrication welding process also generated a non-detected defect or a non-relevant indication that was connected to the lack of fusion defect and the weld surface. This defect corresponds to the rounded dye penetrant surface indication that was not captured by the boat sample. The imperfection may not have been detected by the fabrication surface exams due to the heavy surface grinding, a defect location that was slightly below the weld surface, or a rounded indication size that was acceptable per the code of construction (i.e., < 3/16" diameter). A review of the original fabrication records indicated grinding was performed on all four weld passes for the #68 CRDM, which suggests there were some difficulties in fabricating the periphery tube weld.
- During service, the rounded surface connected defect allowed primary water to enter the tight crevice formed by the sub-surface lack of fusion defect. The combination of the wetted crevice environment, a susceptible tube microstructure, and a high hoop stress from the welding process allowed PWSCC to initiate. Without a surface connected flaw that allowed for wetting of the lack of fusion crevice, the PWSCC would not have initiated at this time.

### **3.0 Laboratory Test Plan**

A laboratory test plan was developed with the assistance of industry materials experts from Exelon Nuclear, EPRI, Westinghouse, Framatome, and several nuclear utilities. The test plan is provided in Appendix A to this report. Due to radioactive contamination, the laboratory evaluations were performed at the BWXT, Inc. facility in Lynchburg, Virginia. The work was performed under Exelon PowerLabs–BWXT Purchase Order 00059971-0001-2007040335. The laboratory testing was observed by Exelon PowerLabs, Exelon Nuclear Corporate Engineering, and Mr. Jai Brihmadesan who is a technical consultant for Exelon Nuclear.

### **4.0 Laboratory Pre-Sectioning Evaluations**

#### **4.1 Visual Inspections**

The as-received boat sample is shown in Figures 4 and 5. The sample measured approximately 1.5” long x 0.75” wide and had a maximum thickness of 0.375”. In this report, the sample directional descriptions (e.g., up, down, left, right) will be referenced as viewing the non-cut (i.e., wetted) surface that is shown in Figure 4.

The visual inspections did not identify cracking or other linear indications that corresponded to the field dye penetrant indications. The most significant observation was the presence of heavy surface grinding toward the upper half (i.e., weld side) of the sample. Due to the surface grinding, the weld toe could not be identified by the visual inspection. The EDM surface exhibited smooth, rounded features that were typical of the EDM cutting process.

#### **4.2 Fluorescent Dye Penetrant Results**

The fluorescent dye penetrant results are shown in Figures 6 and 7. The upper left portion of the sample contained a linear indication that bled heavily on both the wetted and EDM cut surfaces. The indication measured approximately 0.18” long on the non-cut surface and 0.375” long on the EDM surface. Although the indication was not continuous around the upper edge of the EDM cut, a subsequent dye penetrant exam confirmed the two linear indications were connected. Both linear indications were visible in the second exam, even though the fluorescent dye was only applied to the EDM surface. The location and orientation of the linear indications corresponded to the axial indication that was identified by the field NDE inspections (i.e., the axial indication in Figure 2 and Indication #2 in Figure 3).

The fluorescent dye penetrant examination also detected a single rounded indication on the EDM surface. The rounded indication was located approximately 0.090” from the axial indication.

#### **4.3 Laboratory Microfocus Radiography**

The boat sample was examined using BWXT’s real-time Microfocus X-ray system. The examination detected the axial indication that was identified by the fluorescent dye penetrant testing; although, no other indications were detected. Figure 8 contains a montage of the boat sample X-ray results.

#### 4.4 Stereoscope Examinations

The boat sample surfaces were examined using a stereoscope, with particular emphasis on the dye penetrant indications. Due to surface grinding marks, the axial indication could not be identified by the stereoscope inspection of the non-cut surface (Figure 9). The axial indication was detected on the EDM surface (Figure 10).

A stereoscope inspection was also performed at the rounded indication on the EDM surface. However, the defect characteristics were obscured by globular debris from the EDM cutting process.

#### 4.5 Surface Scanning Electron Microscope (SEM) Examinations

A low magnification SEM view of the non-cut surface is shown in Figure 11. On the non-cut surface, the axial indication was relatively tight and could only be detected at high magnifications. The indication followed a non-branching irregular path that did not necessarily coincide with the local grinding marks (Figures 12 & 13). In one region, the indication coincided with a local patch of ductile features, which appeared to be related to smeared metal from the surface grinding (Figure 14). No crack branching was observed on the non-cut surface.

During the SEM inspections of the non-cut surface, several angled fissures were also detected (Figures 15). The fissures tended to follow to the local grinding direction.

The axial indication was easily detected by the SEM examination of the EDM surface (Figure 16). Figures 17 and 18 provide typical views of the crack. There was little crack branching, except near the ends of the indication.

The Figure 17 photo also provides a view of the rounded dye penetrant indication on EDM surface. As was reported during the stereoscope inspection, the indication features were obscured by globular debris from the EDM cutting process.

### 5.0 Laboratory Sectioning Plan and Sample Identifications

The laboratory NDE results indicated the upper left portion of the boat sample in Figure 4 contained the axial indication that was detected by the field NDE inspections. The boat sample also contained a rounded indication on the EDM cut, which corresponded to a portion of the angled, sub-surface indication that was uncovered by the boat sample removal (Indication #3 in Figure 3).

A boat sample sectioning plan was developed to allow for metallurgical characterization of the two indications and to perform the remaining evaluations that were identified in the test plan. The boat sample sectioning details, sample identifications, and planned examinations are summarized in Figures 19 and 20.

### 6.0 Sample C Macro-Etch Results

The Section C cut face was lightly ground and macro-etched as shown in Figures 21 and 22. The etching revealed the boat sample contained portions of the last two weld passes. Based on the profile

of the wetted surface of the tube, there was minor surface grinding of the tube near the toe of the weld.

## **7.0 Sample B Metallography**

The horizontal cut that separated Samples A and B was approximately 0.23" from the upper EDM edge. The cut location was below the axial indication on the wetted surface of the boat sample, but intersected the axial indication on the EDM surface.

The horizontal cut face on Sample B was prepared in a metallurgical mount. The tube base metal contained branched, intergranular cracking (Figures 23-25) that was typical of PWSCC. The crack branches had sharp tips and contained little oxidation. No crack blunting was observed. There was limited interdendritic cracking into the weld (Figure 26). Within the Sample B mount, none of the cracking extended to the wetted surface of the boat sample.

The surface of the weld exhibited an irregular contour and several linear indications were observed (Figure 27 – 29). Based on the heavily deformed surface microstructure, the linear indications appeared to be laps that were formed by metal deformation during grinding. In the examined section, the deformed layer measured up to 0.0007" thick. There was no evidence of service related crack initiation from the indications. The deformed metal and local crevices are believed to be the source of the fissures that were detected by the SEM examination of the wetted surface.

The tube material had a relatively fine duplex grain structure with the smallest grains measuring ASTM Size 7 and the largest grains ASTM Size 5. The microstructure contained large quantities of random intragranular carbides and the grain boundaries were partially decorated with carbides (Figure 30). Nuclear industry literature indicates this microstructure will have a relatively high susceptibility to PWSCC (Ref. 4, 5). The microstructure is considered typical for mill annealed Alloy 600 tubing that was fabricated during the 1970's.

## **8.0 Sample A1, Crack Surface Examinations**

The axial indication was exposed by bending and the Sample A1 side of the crack is shown in Figure 31. The crack surface was reflective and appeared intergranular. There were no clear indications of crack age; although, a thumbnail-shaped region on the tube appeared to be more oxidized than the remainder of the sample.

A low magnification SEM view of the A1 crack surface is shown in Figure 32. The general shape of the thumbnail region in the vicinity of the fusion line suggested the direction of crack propagation was from the tube material into the weld (i.e., toward the wetted surface of the J-groove weld along the tube side fillet leg). The tube portion of the sample exhibited an intergranular morphology in all examined regions (Figures 33-35). A close examination of the 'thumbnail' region revealed fine globular particles on the surface. Several of the particles were evaluated by energy dispersive X-ray spectrometry (EDS) techniques and found to contain tungsten, oxygen and the base metal elements (i.e., nickel, chromium, iron). As a result, it was concluded that the thumbnail region was contaminated during the EDM cutting process.

The exposed surface of the weld exhibited several characteristics. At low magnification, the weld

cracking appeared to follow the columnar interdendritic features of the solidification pattern (Figure 36), which is typical of stress corrosion cracking. However, at higher magnifications, some of the features were smoother than is typical for PWSCC (Figure 37 & 38). Industry literature indicates the smooth interdendritic features are more indicative hot cracking than PWSCC (Ref. 6). Several of the smooth regions were evaluated by EDS techniques; however, the areas did not exhibit manganese segregation that can be associated with hot cracks. Based on the crack surface features, it was concluded that there was evidence of both PWSCC and hot cracking in the weld.

The exposed weld surface also contained a planar defect that was parallel to the fusion line (Figures 39 & 40). Based on defect location and orientation, the defect was caused by lack of fusion between weld passes. Within the weld, there were several cracks that were connected to the defect.

Various portions of the weld contained local patches of dimpled voids, which are indicative of ductile tearing (Figure 41). The tearing may have occurred during service PWSCC propagation due to residual stresses from the welding process, but it is also possible the regions were small intact ligaments that failed when the crack surface was broken open in the lab. In general, there were more ductile tearing regions toward the wetted surface of the sample.

Based on the general characteristics of the weld defects, interdendritic weld separations, direction of crack branching, and local ductile tearing, it was concluded that the primary direction of cracking within the weld was toward the wetted surface of the boat sample. This suggests the PWSCC did not initiate from the wetted surface of the boat sample.

## **9.0 Sample A2A Evaluations**

The Section A2A axial cut was located approximately 0.040" from the rounded dye penetrant indication on the EDM surface. The cut face was placed in a metallurgical mount and multiple grind-polish-examine steps were performed until the indication was uncovered. The indication was identified as a weld lack of fusion defect between the surface of the tube and the weld (Figures 42-44).

The metallurgical sample was re-polished in preparation for an SEM exam. The polishing step uncovered a porous inclusion near the edge of the lack of fusion crevice (Figure 45). Several incipient interdendritic cracks had initiated from the edge of the inclusion and the lack of fusion crevice (Figures 46 & 47). Most of the cracks appeared to be hot cracks; however, the angular appearance of two indications appeared similar to incipient PWSCC.

Qualitative EDS evaluations were performed on the large inclusion, the material in the lack of fusion crevice, several small inclusions that were adjacent to the crevice, and the oxide within several cracks. A general dot map scan of the elements was also performed. The results are summarized below.

- The large inclusion and most of the smaller inclusions contained titanium, nitrogen, and oxygen, which suggests they were titanium nitrides or oxides. One very small weld metal inclusion contained calcium and fluorine, which was likely related to the welding flux.
- The lack of fusion crevice contained oxidized metallic particles from the EDM wire and base metal cutting debris (i.e., tungsten, oxygen, iron, nickel, chromium and niobium).

- The material within the incipient cracks was consistent with Inconel 182 weld metal oxidation products.
- No measurable fluorine or other potentially corrosive elements were identified in the incipient cracks or the lack of fusion crevice.

After the SEM evaluations, additional grinding was performed to determine if the lack of fusion crevice continued toward the axial crack. However, the lack of fusion defect rapidly disappeared after another grinding sequence. Within the boat sample, the lack of fusion defect measured approximately 0.032” long, which indicates that only a small portion of the angled, sub-surface defect was captured by the boat sample.

The remaining Sample A2A metal was removed from the mount and re-oriented in a new metallurgical mount. The sample was positioned so the axial crack was perpendicular to the mount face, with the upper portion of the EDM cut parallel to the mount face. The primary objective for the mount was to determine if the lack of fusion defect continued toward the axial crack within the mount. The re-oriented mount was evaluated at three locations within 0.013” of the EDM surface. No lack of fusion or other anomalies were identified.

The grinding continued for another 0.094” on the re-oriented sample and the weld edge is shown in Figures 48 and 49. There was limited crack branching within the weld. The tube cracking exhibited intergranular features (Figure 50).

## 10.0 Chemistry Results

The boat sample size did not allow for a full chemical analysis of the weld metal. As a result, the weld chemistry was measured by energy dispersive X-ray spectroscopy (EDS), which is not capable of accurately measuring small quantities of elements that may be specified (e.g., carbon, sulfur). The weld chemistry was evaluated near the middle of the weld on the sample A2A metallurgical mount and the results are summarized in Table 1. Based on the EDS results, the weld chemistry was consistent with Inconel 182 filler metal.

Table 1 – Weld Chemistry Measured by EDS Techniques (Wt.%)

Element	Weld
Nickel	67.18
Manganese	6.67
Iron	8.56
Silicon	0.64
Chromium	14.80
Titanium	0.49
Niobium	1.66

The tube chemistry was analyzed by inductively-coupled-plasma spectroscopy (ICP) and Leco combustion techniques. The results are provided in Table 2 along with the fabrication test report for

Heat 80054 tubing. The tube chemistry was consistent with the fabrication records.

Table 2 – Tube Chemistry Results and Babcock & Wilcox Test Report for Heat 80054 (Wt.%)

Element	Tube	Heat 80054
Carbon*	0.023	0.029
Manganese	0.14	0.27
Sulfur*	0.002	0.002
Phosphorus	< 0.005	--
Silicon	0.35	0.29
Chromium	16.24	16.30
Nickel	76.0	76.32
Copper	0.009	0.02
Cobalt	0.046	0.007
Iron	6.68	6.30
Aluminum	0.17	--

\*Carbon and sulfur were measured by Leco combustion techniques. The remaining elements were measured by ICP.

### 11.0 Microhardness Testing

Microhardness measurements were performed at several areas of interest in the sample B metallurgical mount and the results are reported in Table 3. The results can be summarized as follows:

- The equivalent weld hardness values ranged from 89.7 Rockwell B (HRB) to 98.6 HRB in areas away from the ground (cold worked) surface. The weld hardness in the cold worked surface layer was between 21.2 Rockwell C to 25.3 HRC.
- The equivalent tube hardness measurements were between 82.0 HRB and 88.1 HRB. In general, the higher measurements were located toward the outer diameter of the tube.

Other than the relatively high hardness on the cold worked surface layer of the weld, the measurements are considered typical for the fabrication materials (i.e., mill annealed Alloy 600 tubing and Inconel 182 weld metal).

Table 3 – Knoop Microhardness Results and Equivalent Rockwell Scale Hardness\*

Location	Knoop Measurements	Equivalent Rockwell Hardness Range
Weld Metal (Area 1)		
- Away from Deformed Surface Layer	HK = 259.1, 271.7, 226.6, 224.3, 234.2	91.7 HRB to 98.6 HRB
- In Deformed Surface Layer	HK = 286.4, 274.8, 290.8	21.2 HRC to 23.6 HRC

Weld Metal (Area 2)		
- Away from Deformed Surface Layer	HK = 213.4, 224.3, 225.0, 245.9, 251.2	89.7 HRB to 96.0 HRB
- In Deformed Surface Layer	HK = 303.1	25.3 HRC
Weld Metal (Area 3)		
- Surrounding weld cracking near fusion line	HK = 223.5, 227.1, 243.3	91.5 HRB to 94.7 HRB
Tube, Near Surface	HK = 195.8, 204.5, 204.5, 203.2, 201.9	86.2 HRB to 88.1 HRB
Tube, Away from Surface	HK = 201.9, 181.3, 195.2, 185.2, 180.2	82.0 HRB to 87.6 HRB

\*The microhardness measurements were performed at approximately 0.010" increments in the areas of interest with a 500 gram load. The equivalent Rockwell hardness values were obtained from ASTM E140, Conversion Table 3 for nickel alloys.

## 12.0 Fabrication Records

The Byron Unit 2 reactor head was fabricated at the Babcock & Wilcox, Mt. Vernon, Indiana shop in 1977. The applicable code was the 1971 Edition of the ASME Section III, Summer 1973 Addenda. The fabrication summary that is documented in Reference 7 indicates the #68 CRDM nozzle for Byron Unit 2 came from material Heat 80054. The nozzle tube was supplied by the Babcock & Wilcox Tubular Division in accordance with ASME Section II, Part B, SB-167. The reported mechanical properties for Heat 80054 were 94.6 ksi tensile, 36.5 ksi yield strength, and 48% elongation. The Heat 80054 material was used in 26 penetrations on Byron Unit 2 and three penetrations on Braidwood Unit 2.

The Reference 7 summary reported that the CRDM J-groove welds were fabricated with four passes. The #68 penetration was a periphery tube and the axial indication was located 16.5 degrees from the downhill side of the weld. For the #68 penetration, grinding was performed on all four weld passes to remove indications, which suggests there were some difficulties in fabricating the #68 penetration weld. No weld repairs were reported for the #68 penetration. There were no available fabrication records that mapped out the grinding excavations or the dye penetrant results for the individual weld layers. Per the 1971 edition of ASME Section III, NB-5000, an isolated 3/16" long rounded dye penetrant indication would be acceptable.

## 13.0 Discussion of Results

Based on the information provided by the site in Reference 8, Byron Unit 2 had accumulated 2.219 effective degradation years (EDY) at the end of cycle 13. Since the accumulated EDY categorizes Byron Unit 2 as low susceptibility PWSCC plant per NRC Order EA-03-009, it is unexpected to have identified PWSCC at this time.

The three factors that control PWSCC are material susceptibility, stress and corrosion environment. Based on the microstructure in the boat sample materials (i.e., random intragranular carbides and partially decorated grain boundaries), the tube material had a relatively high susceptibility to PWSCC. However, the observed microstructure and material susceptibility were not considered unusual for mill annealed Alloy 600 tubing produced during the 1970's. As a result, the tube microstructure and material susceptibility were not considered the cause for early PWSCC initiation. This conclusion is supported by the fact that no other cracking was detected by the ultrasonic inspections of the other 28 penetrations in Exelon plants that were fabricated from Heat 80054 tubing.

The Reference 9 document contains multiple stress analyses for the Byron Unit 2 CRDM penetrations. A hoop stress plot for the configuration of the #68 penetration is shown in Figure 51. The plot combines the residual welding and operating pressure stresses. There are three high stress regions on the tube, where the calculated hoop stress is between 50 to 100 ksi. One high stress region is located on the outer diameter of the tube near the downhill side of the J-groove weld, which is the approximate location of the axial cracking. No cracking was detected at the other two high stress locations, which suggests that an atypical environment may have existed at the axial crack location.

The lab evaluations identified welding defects in the form of lack of fusion between weld passes, lack of fusion to the tube, and hot cracks within the weld. The presence of the sub-surface lack of fusion defect is considered the cause of the atypical environment that promoted PWSCC. When wetted, the lack of fusion defect would have generated an atypical crevice corrosion environment that is conducive to PWSCC. Without the lack of fusion defect, the crevice environment would not have been present and PWSCC would not have initiated at this time.

For PWSCC to occur, the Alloy 600 material must be wetted at the crack initiation site. Since the boat sample lab evaluations indicated the general direction of axial cracking within the weld was toward the wetted surface, there must have been another surface connected path for the lack of fusion defect. The field dye penetrant exams detected one other indication on the J-groove weld surface (i.e., the rounded indication that was not captured by the boat sample). As a result, it is likely the rounded surface indication was connected to the angled lack of fusion defect, which intersected the axial indication.

Since the rounded indication was not captured by the boat sample, it was not possible to determine the cause of the defect. However, based on the presence of welding defects in the boat sample, the most probable cause is considered a welding imperfection that was not detectable or an indication that was considered acceptable per the fabrication inspection requirements. This conclusion is supported by the fabrication records, which indicated grinding was required for all four weld passes. Since a final fabrication dye penetrant examination was performed, it is possible the defect was covered by smeared metal from the surface grinding, situated at a non-detectable location slightly below the weld surface, or the dye penetrant indication size was less than the minimum relevant size for a rounded indication. The code of construction would have accepted an isolated rounded dye penetrant indication that was less than 3/16" long.

#### **14.0 Statement of Quality**

Testing was performed with standard equipment that have accuracies traceable to nationally recognized standards, or to physical constants, by qualified personnel, and in accordance with the Exelon PowerLabs Quality Assurance Program revision 18 dated 01/11/2007.

*The internal PowerLabs Project review and approval is electronically authenticated in Exelon PowerLabs project record.*

#### **15.0 - References**

1. Westinghouse Ultrasonic Report Sheet for Byron Unit 2, Penetration 68, File CBE-R13-BP01-68-01, Dated 4/9/2007.
2. Exelon Nuclear Liquid Penetrant Examination Data Sheet Report 2007-276, Dated 4/10/07.
3. Exelon Nuclear Liquid Penetrant Examination Data Sheet Report 2007-315, Dated 4/23/07.
4. EPRI Report 1002792, Materials Handbook for Nuclear Plant Pressure Boundary Applications, December 2002.
5. Microstructural and Mechanical Property Evaluation of Alloy 600 CRDM Nozzles from B&W Design Reactor Vessel Heads, S. Fyfitch, et. al., AREVA NP Inc.
6. Differentiation Between Hot Cracking and Stress Corrosion Cracking in PWR Primary Water of Alloy 182 Weld Material, J.M. Boursier, et. al., Electricite De France.
7. AREVA Engineering Information Record 51-5014160-001, Vessel Head Penet. Nozzle Data For Byron 1 & 2, Braidwood 1& 2, Dated 5/11/07.
8. Exelon Nuclear EC 364572, Rev. 00, Titled B2R13 End of Cycle 13 Effective Degradation Years (EDY) In Accordance With NRC Order EA-03-009.
9. Byron and Braidwood Units 1 and 2 CRDM Stress Analysis, Dominion Engineering, Inc. Task 77-70, Calculation C-7770-00-1, Rev. 0, Dated 4/25/03.

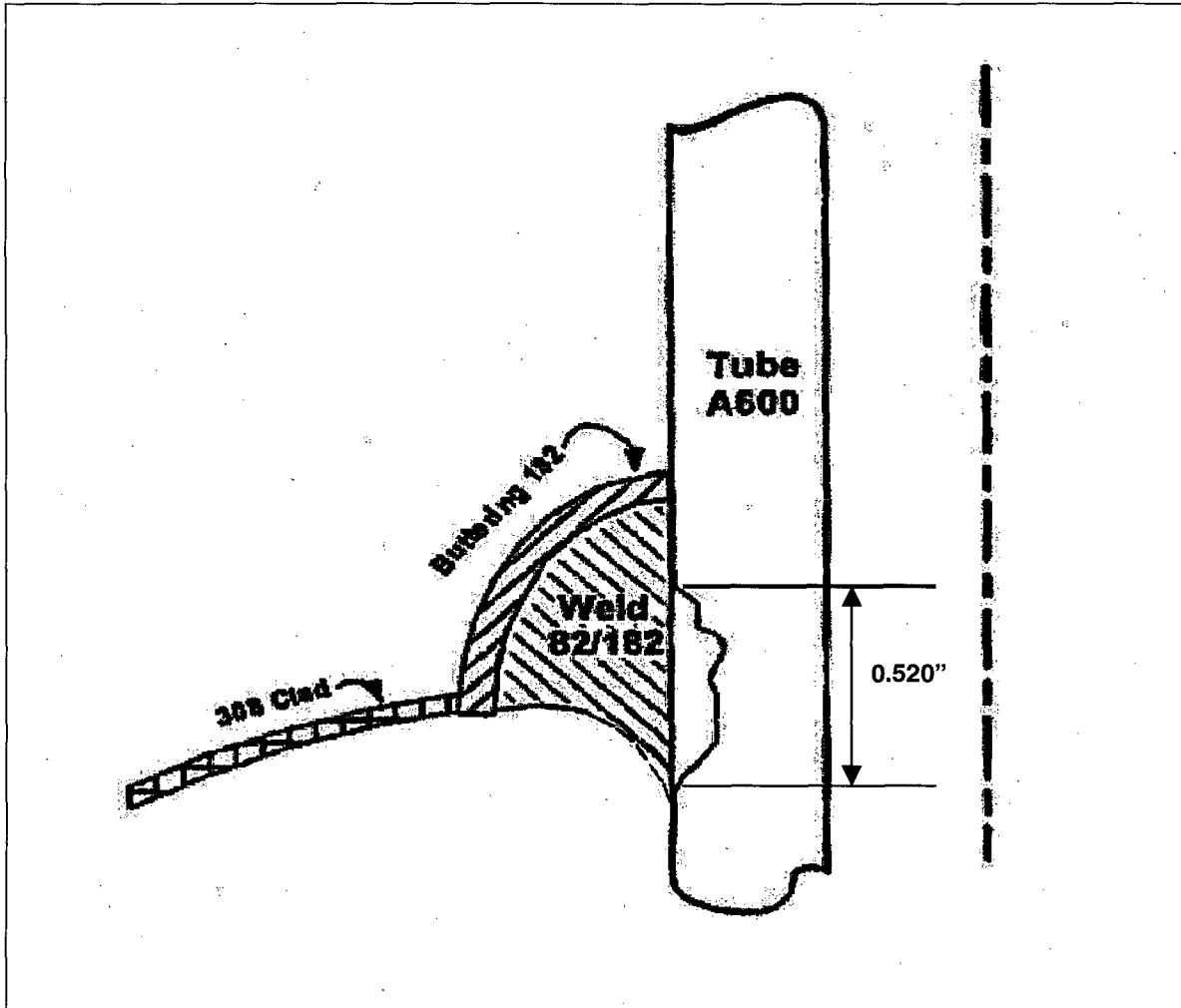


Figure 1 – A non-scale sketch of the ultrasonic indication identified in the Reference 1 report. The inspection identified a 0.520" long x 0.326" deep axial, external indication in the #68 CRDM penetration tube near the J-groove elevation. The 0.326" depth corresponds to approximately 52% of the 0.625" tube thickness. The maximum ultrasonic reflector was approximately 16.5 degrees counter clockwise from the zero reference (as looking upward). The zero reference was the downhill side of the periphery tube. A follow-up eddy current exam detected no relevant indications on the inner surface of the tube.

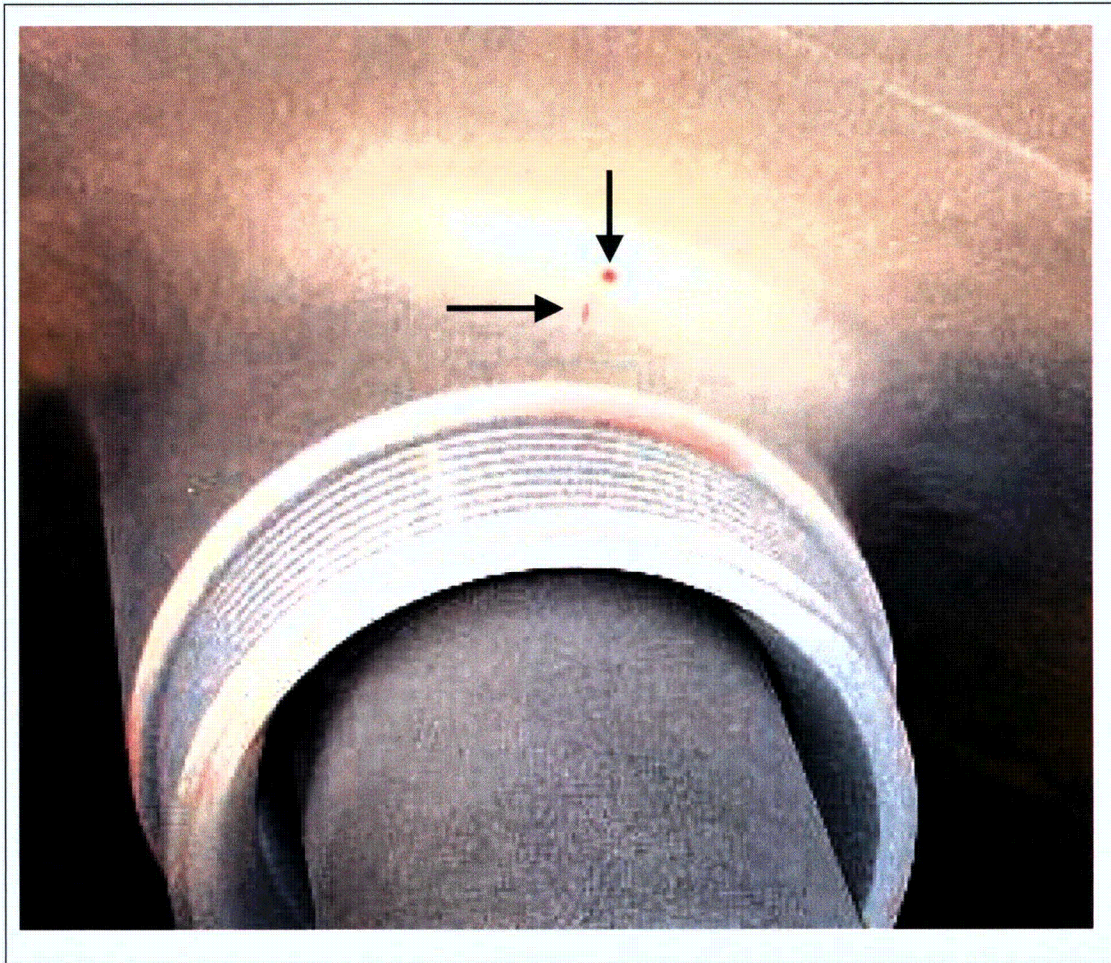


Figure 2 – A photo showing two dye penetrant indications on the surface of the J-groove weld zone for the #68 CRDM penetration (Ref. 2). The axial indication (left arrow) measured 0.150” long and corresponded to the approximate location of the axial ultrasonic reflector. A rounded 0.050” diameter indication was also detected (upper arrow). The lab evaluations indicated the J-groove weld toe was below the axial indication.

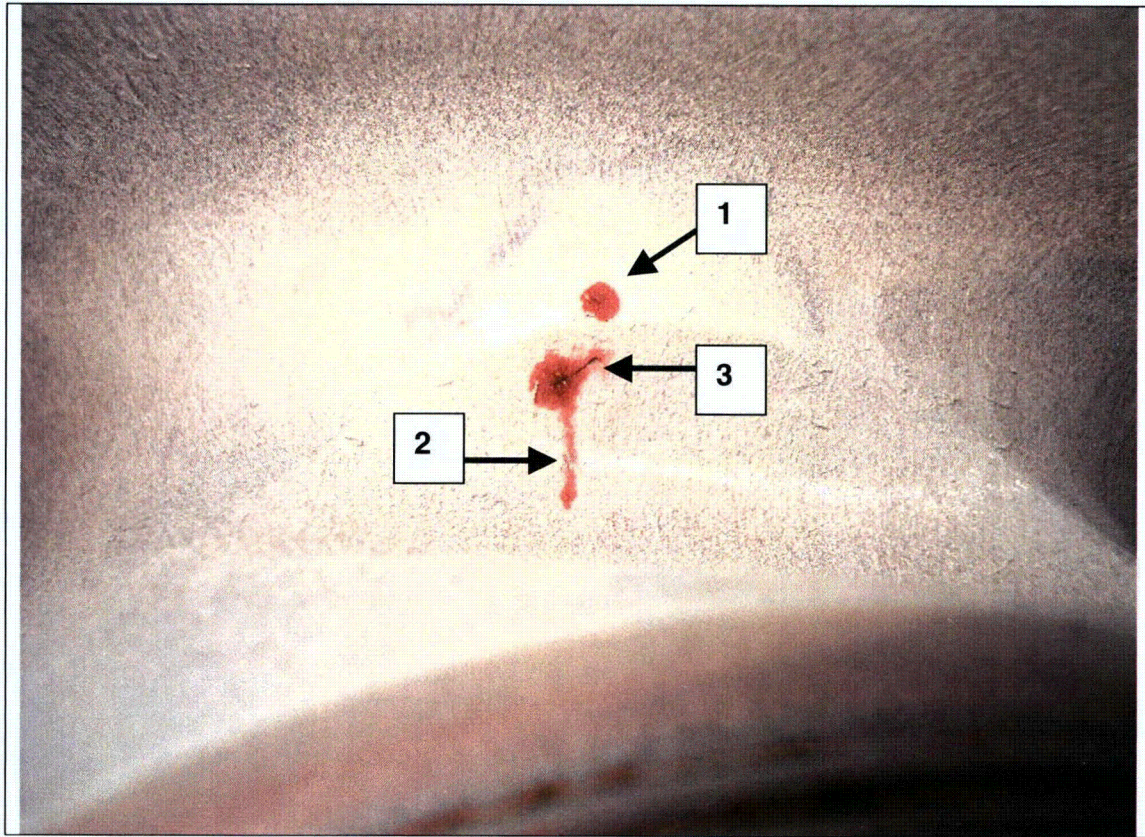


Figure 3 – A photo showing the field dye penetrant results for the excavation site after the boat sample was removed (Ref. 3). The boat sample did not capture the rounded indication (#1) or the deepest portion of the axial indication (#2). In addition, the excavation uncovered an angled, sub-surface linear defect (#3) that intersected the axial indication.



Figure 4 – The non-cut (i.e. wetted) surface of the boat sample. Note the relatively heavy grinding toward the upper half (weld side) of the sample. The sample measured 1.5” long x 0.75” wide. No crack-like indications were visible. (4x Magnification)



Figure 5 – The EDM cut surface. No cracking was visible. (4x Magnification)

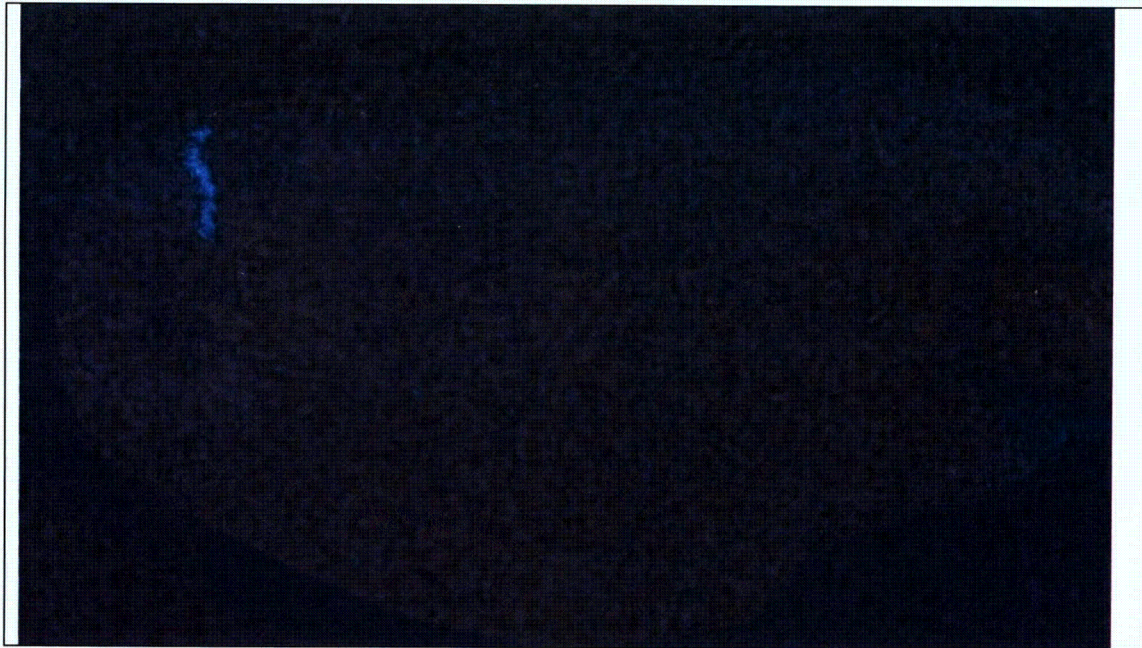


Figure 6 – A photo showing the fluorescent dye penetrant indication on the non-cut surface of the boat sample. The indication measured 0.18” long and followed an irregular path.



Figure 7 – The fluorescent dye penetrant result for the EDM surface. The large indication measured 0.375” long. Also note the smaller rounded indication (arrow).

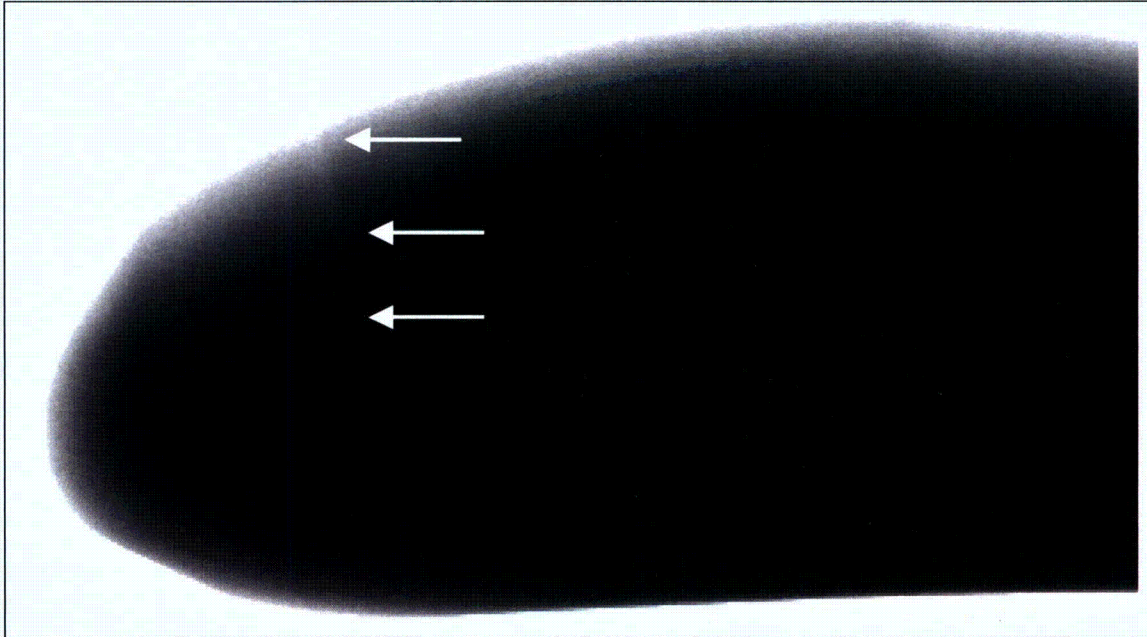


Figure 8 – An X-ray photo with the axial indication highlighted by arrows.

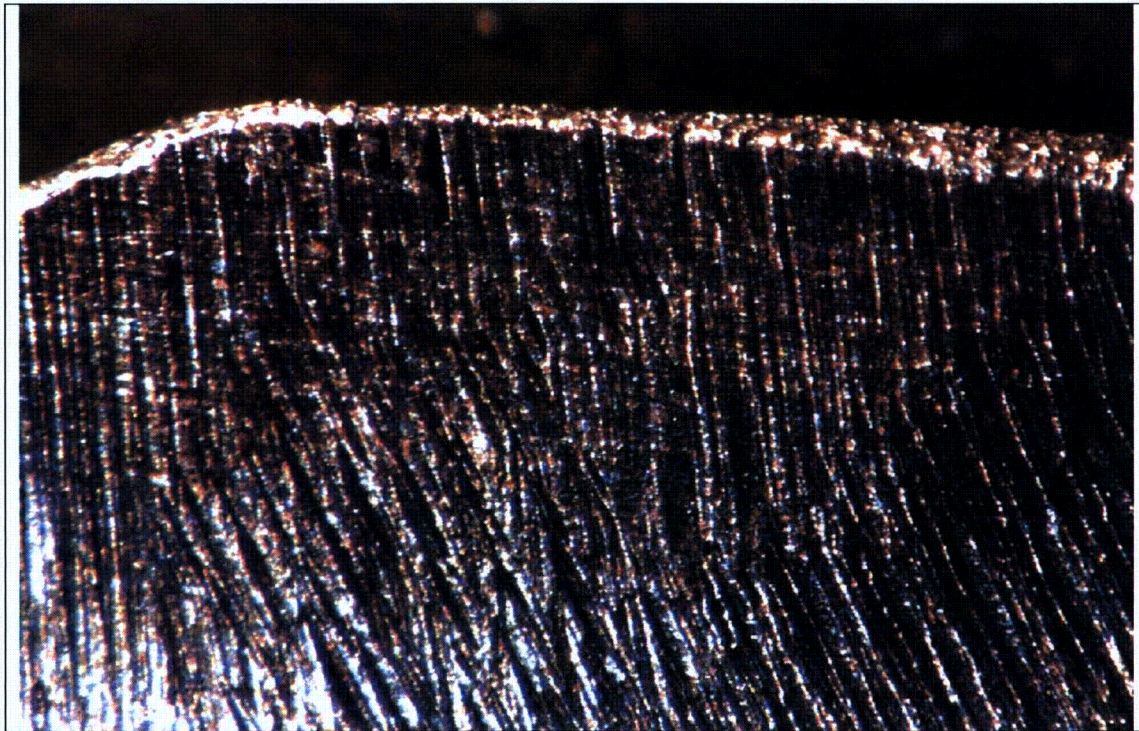


Figure 9 – A stereoscope view in the area of the axial indication region on the non-cut surface. Due to the grinding marks, the indication is not visible. (27x Magnification)

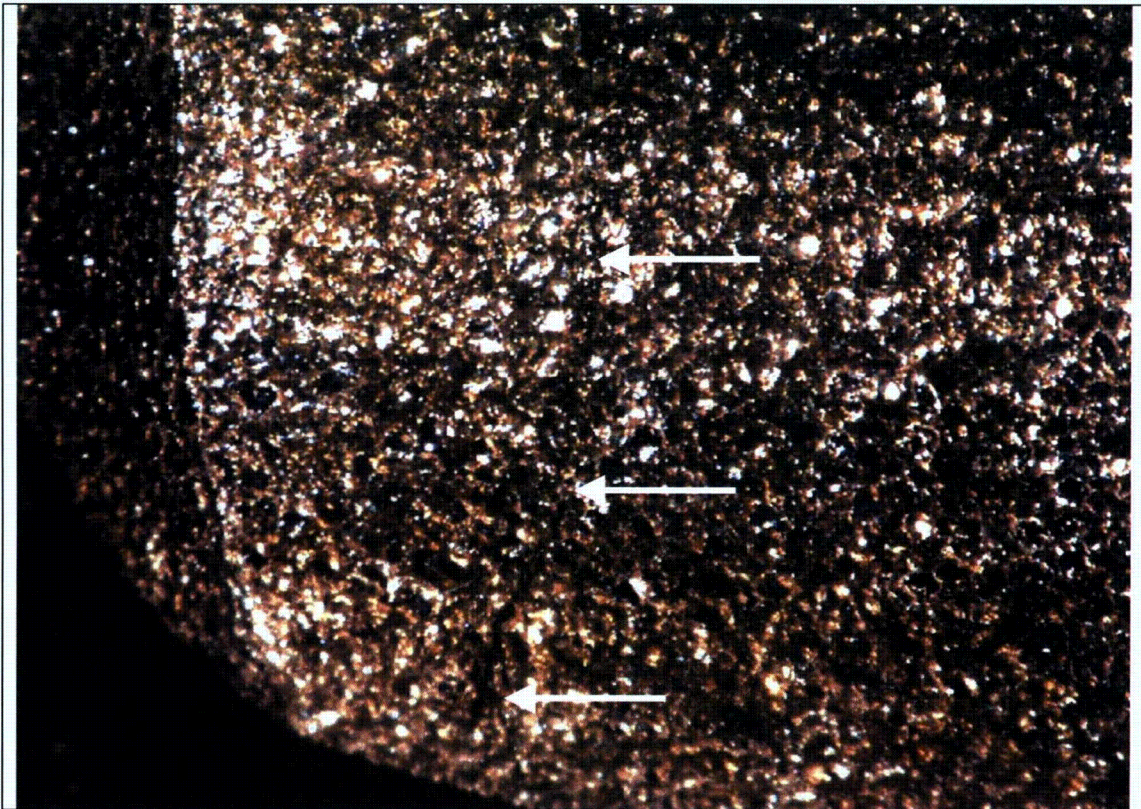


Figure 10 – A stereoscope photo showing the axial crack on the EDM cut surface. (17x Magnification)

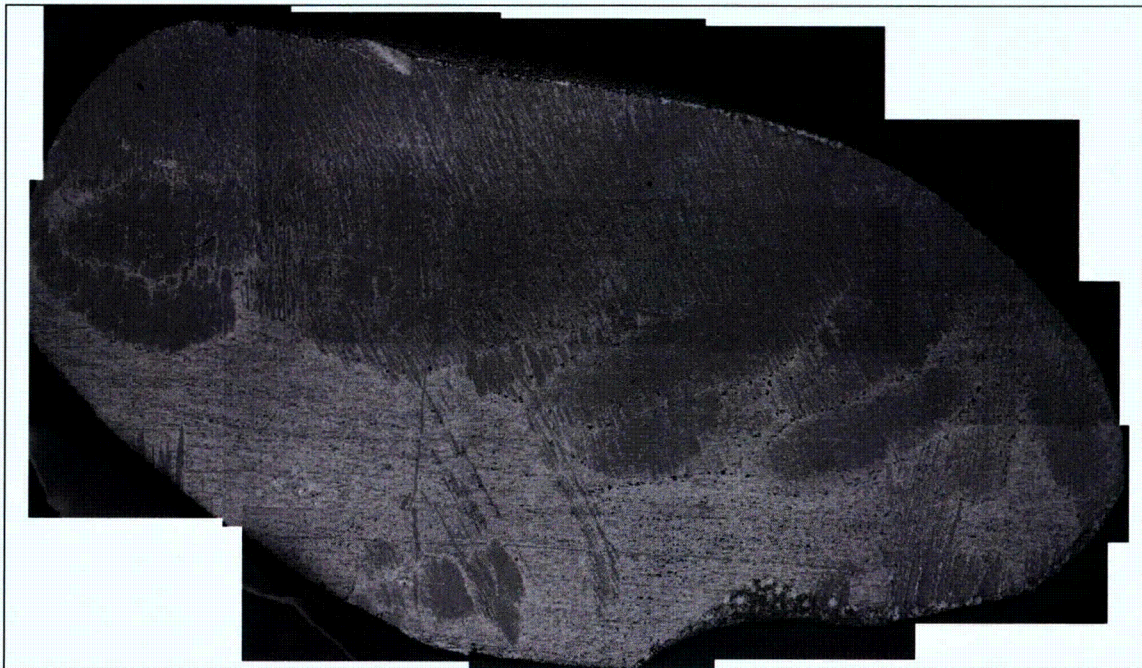


Figure 11 – A low magnification SEM photo of the non-cut surface. (4x Magnification)



Figure 12 – An SEM photo near the upper end of the axial indication on the non-cut surface. There is evidence of smearing from the surface grinding. (500x Magnification)



Figure 13 – An SEM photo of the axial crack on the non-cut surface. The crack followed an irregular path and was non-branching. In this area, the crack did not follow the local grinding marks. (500x Magnification)



Figure 14 – A local patch of ductile appearing dimples (arrows) in the axial indication on the non-cut surface. The dimples were likely related to the surface grinding. In this area the indication followed the grinding direction. (500x Magnification)



Figure 15 – A representative SEM photo showing fissures that were detected on the non-cut surface. The fissures tended to follow the local grinding marks. None of the fissures were detected by the dye penetrant examination. (500x Magnification)

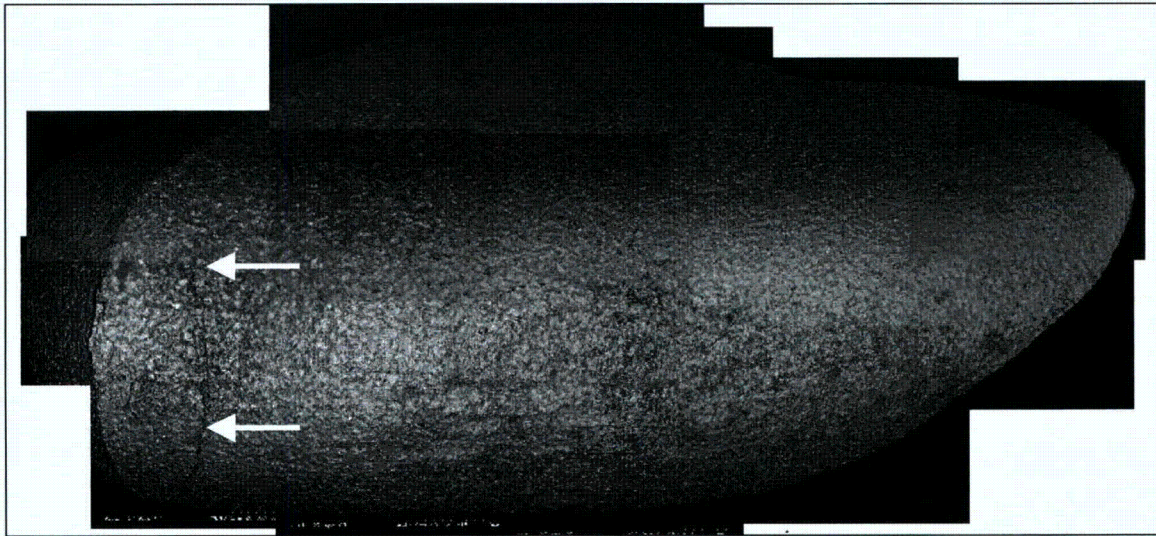


Figure 16 – A backscatter SEM montage of the EDM cut surface. The arrows point to the crack. (4x Magnification)

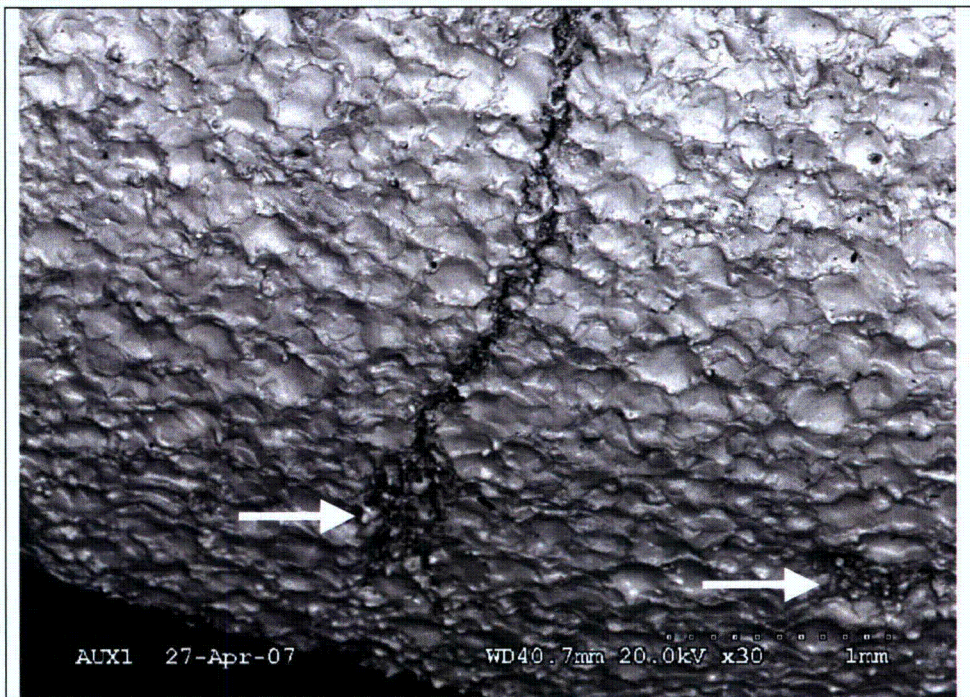


Figure 17 – An SEM photo near the upper end of the axial indication on the EDM surface. The left arrow points to crack branching near the non-cut surface edge. The right arrow points to the globular particles that covered the rounded dye penetrant indication. (30x Magnification)

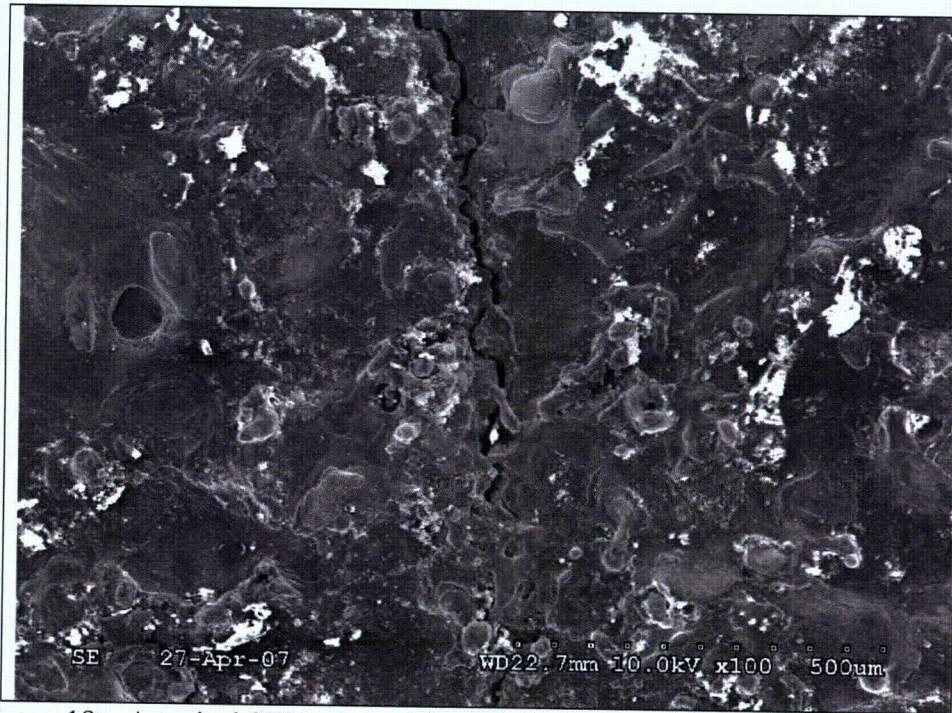


Figure 18 – A typical SEM view of the axial indication on the EDM surface. The crack generally appeared to have intergranular features, although interpretation was difficult due to the EDM process. (100x Magnification)

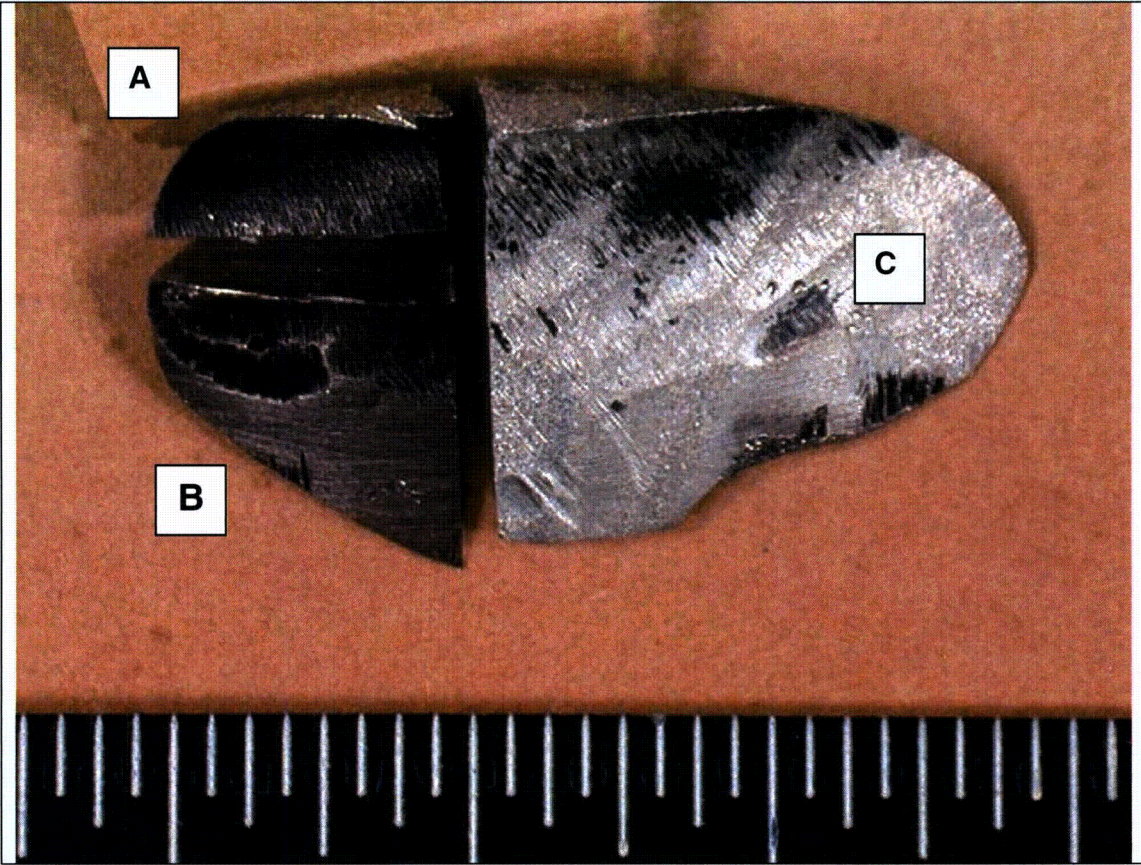


Figure 19 – A photo showing the initial boat sample cuts. The horizontal cut between samples A and B was located approximately 0.050” below the tip of the axial indication. Planned work includes:

- Sample A: Additional sectioning as shown in Figure 20.
- Sample B: Metallography of horizontal cut face. Microhardness testing
- Sample C: Macro-etch cut face to ID weld location. Chemical analysis of tube.

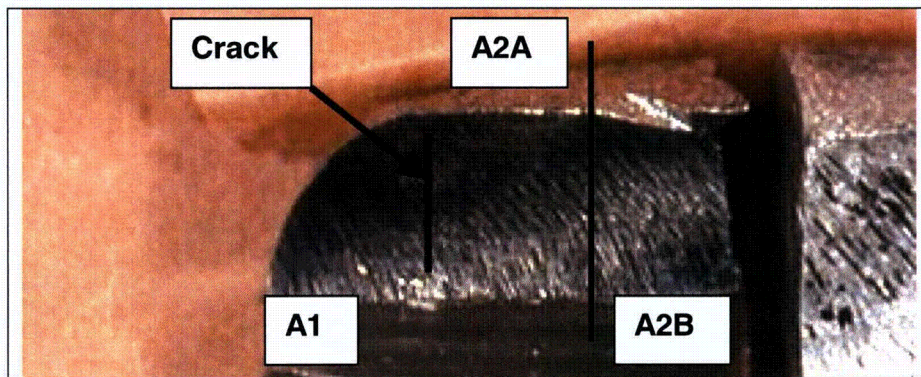


Figure 20 – The sub-sectioning and work plan for Sample A.

- Sample A1: Expose crack surface and examine with stereoscope and SEM
- Sample A2: Metallurgy mounts on lab A2A/A2B cut face and EDM cut surface
- Sample A2B: No work planned

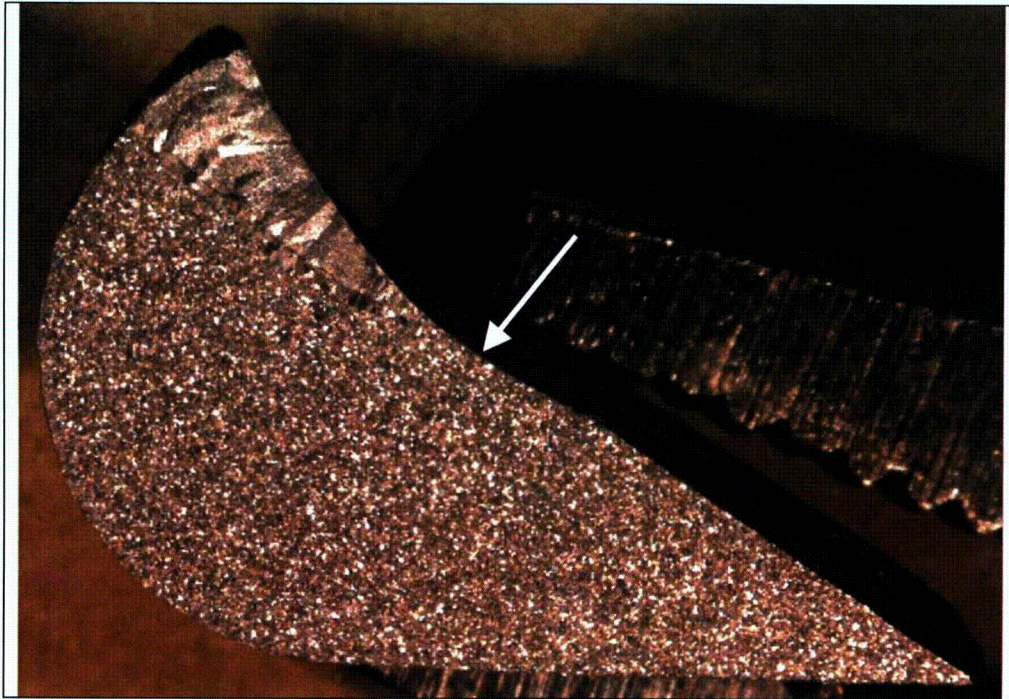


Figure 21 – A macro-etched view of the Sample C cut face. The arrow points to the location of the weld toe on the wetted surface of the boat sample. The tube profile indicates there was minor grinding past the weld toe. (7x Magnification)

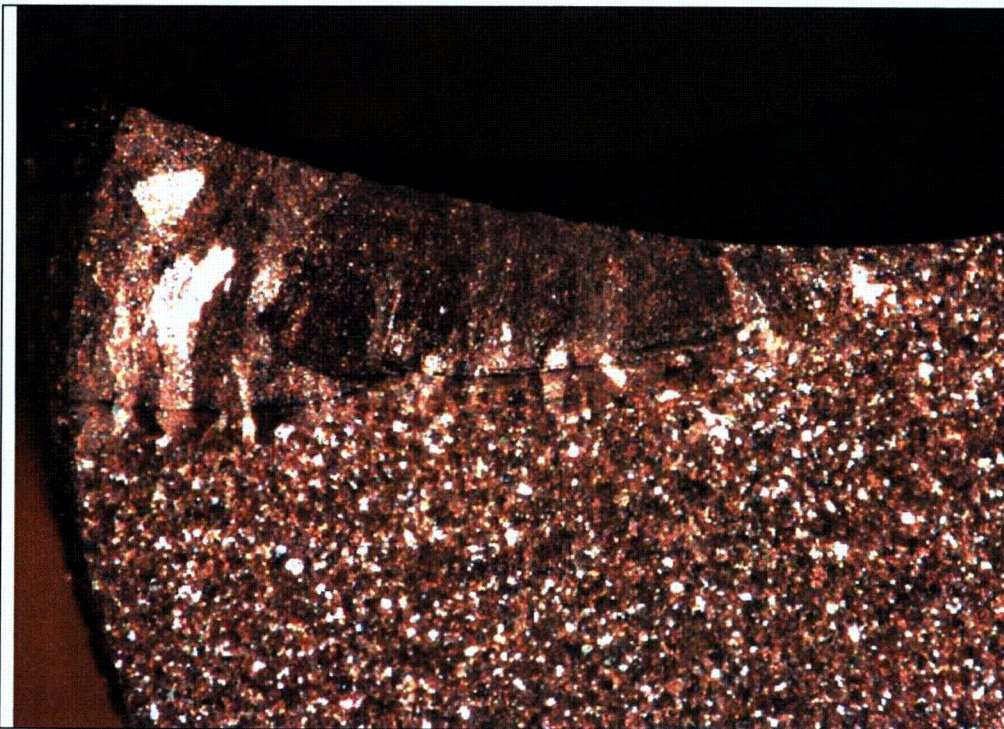


Figure 22 – A closer look at the macro-etched weld. The boat sample contained portions of the last two weld passes. (15.2x Magnification)

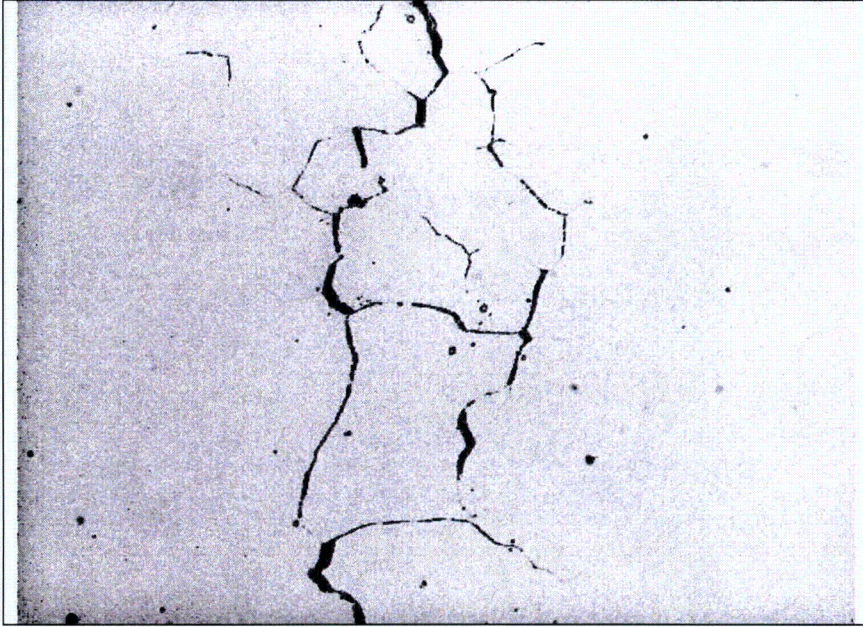


Figure 23 – An un-etched view showing branched, intergranular cracking in the tube portion of the Sample B metallurgical mount. (375x Magnification)

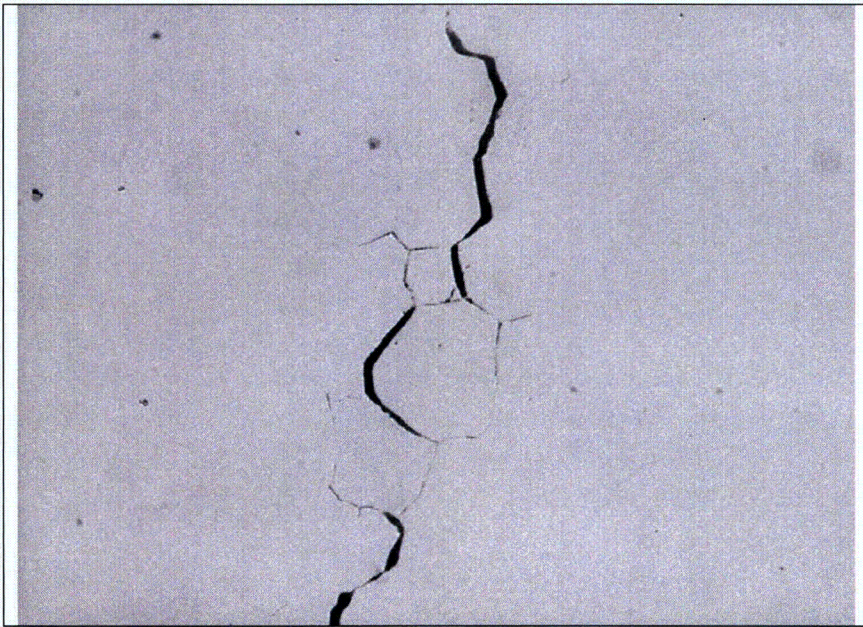


Figure 24 – Additional branched, intergranular cracking in the Sample B tube material. (375x Magnification, Un-etched)

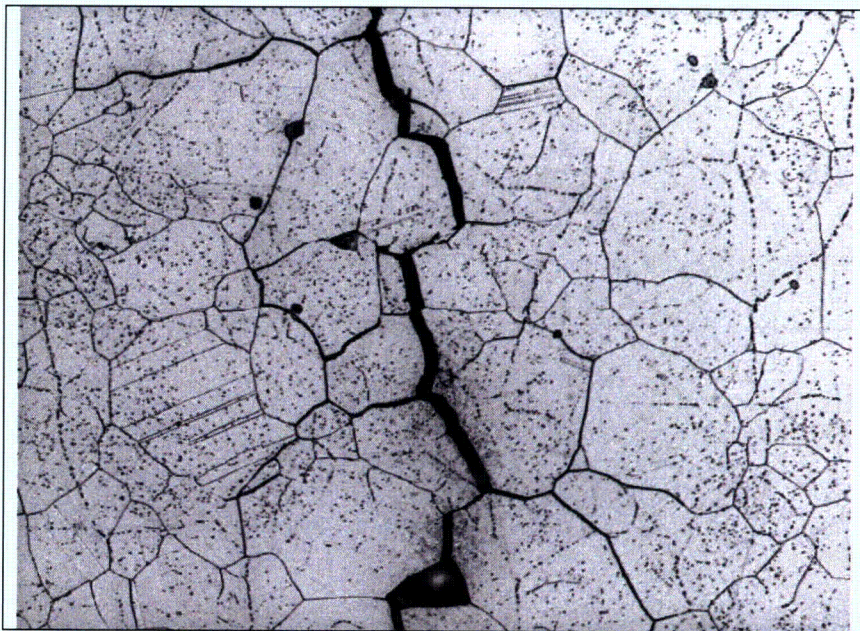


Figure 25 – An etched view of the branched, intergranular cracking in the Sample B tube material. (375x Magnification, Electrolytic Phosphoric-Nital Dual Etch)



Figure 26 – An etched view near the weld metal crack end in Sample B. The two cracks have an intergranular appearance. Within Sample B, the cracking did not extend to the wetted surface of the mount. (375x Mag., Electrolytic Phosphoric-Nital Dual Etch)



Figure 27 – An un-etched view of two linear irregularities on the weld surface in the Sample B mount. (375x Magnification)

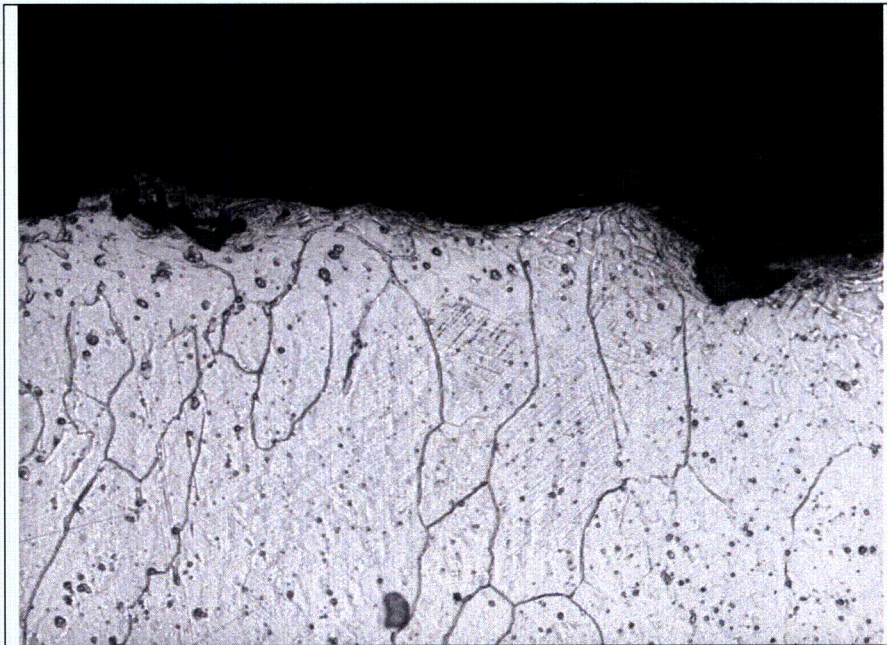


Figure 28 – An etched view of the Figure 27. The locally deformed microstructure suggests the indications were laps from surface grinding. (375x Mag., Electrolytic Phosphoric-Nital Dual Etch)

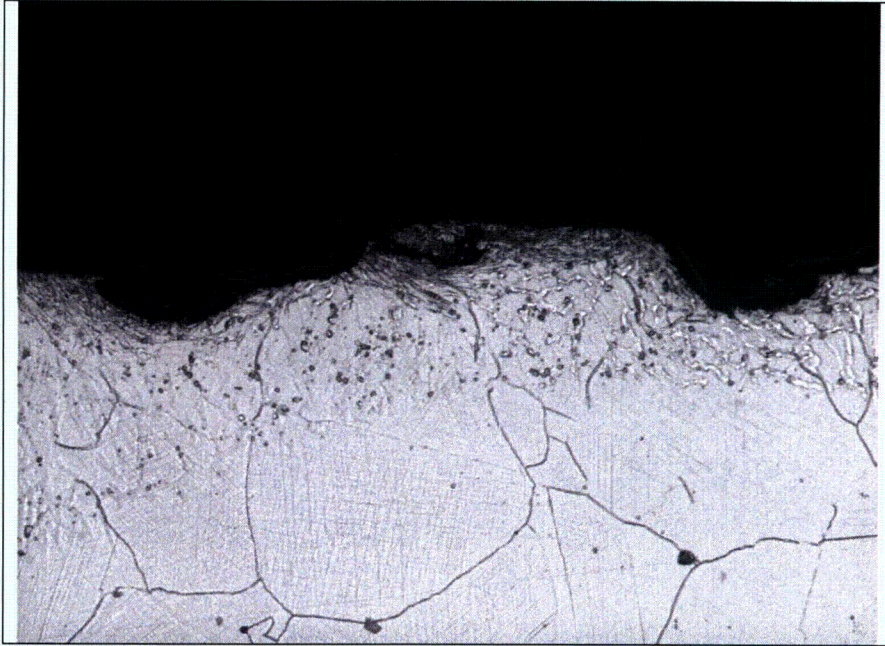


Figure 29 – Another surface indication in the Sample B mount. There was no evidence of crack extension from any of the surface indications. (375x Mag., Electrolytic Phosphoric-Nital Dual Etch)

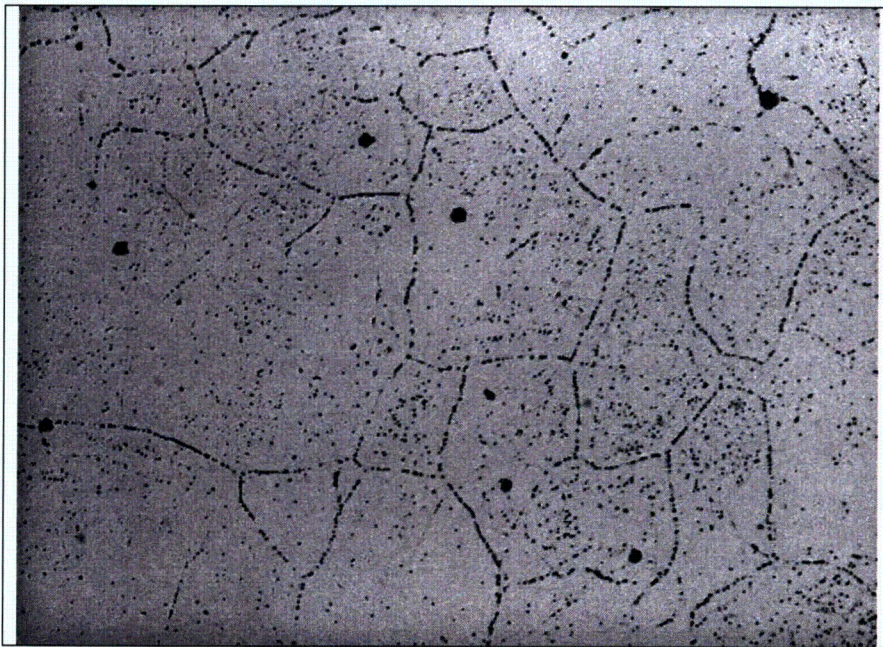


Figure 30 – The Sample B tube material with an electrolytic phosphoric acid etch to reveal the carbide structure. The tube microstructure contained significant intragranular carbides and partially decorated grain boundaries. (375x Magnification)



Figure 31 – A stereoscope view of the exposed surface of the axial crack in Sample A1. The weld is toward the left side of the sample. The crack surface was reflective and had an intergranular/interdendritic appearance. The arrows point to the edge of a thumb-nail-shaped region that appeared to be more oxidized than the remainder of the surface.

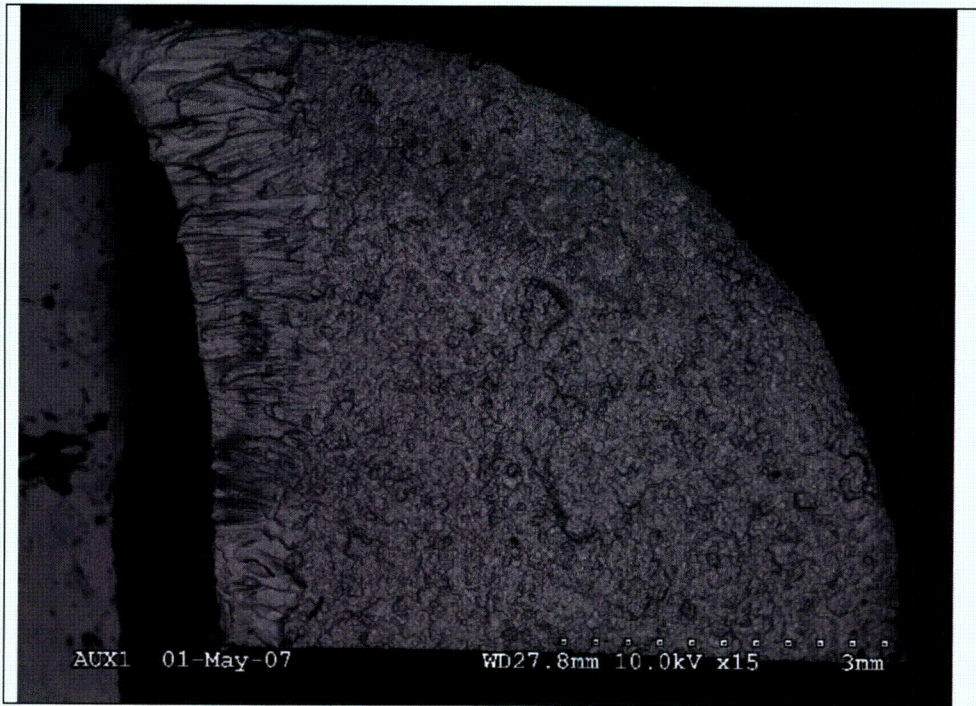


Figure 32 – A low magnification backscatter SEM view of the Sample A1 crack surface with the weld along the left edge of the sample. The ‘thumbnail’ region is also visible. (15x Mag.)



Figure 33 – A typical SEM view of the tube crack surface in the Sample A1. The tube material exhibited intergranular features throughout the sample. (100x Magnification)



Figure 34 – A backscatter SEM image of the intergranular cracking in the dark ‘oxidized’ region in the Figure 31 stereoscope photo. An EDS evaluation indicated the fine globular particles contained tungsten, which suggests the surface was contaminated with debris from EDM cutting process. (300x Magnification)



Figure 35 – The lower portion of the exposed crack surface in Sample A1. The left side of the sample is intact weld metal that was broken open in the lab. The large grained area near the center of the photo was located in the base metal heat affected zone. (100x Magnification)

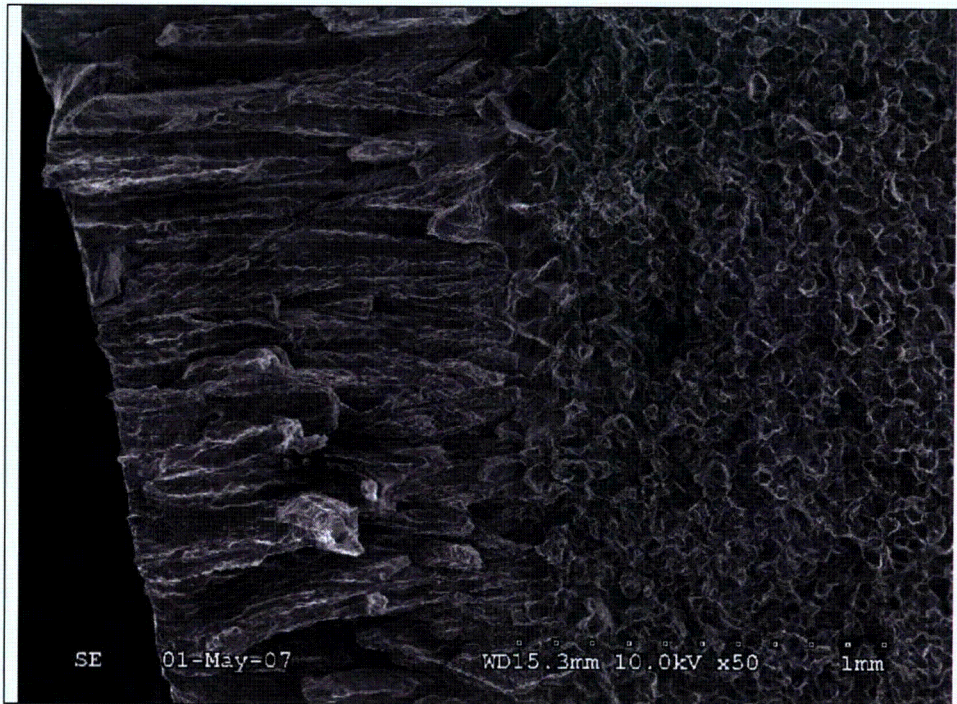


Figure 36 – An SEM photo near the center of the exposed crack in the sample A1 weld. At low magnification, the weld cracking appeared to follow the columnar, interdendritic features of the weld solidification pattern. (50x Magnification)

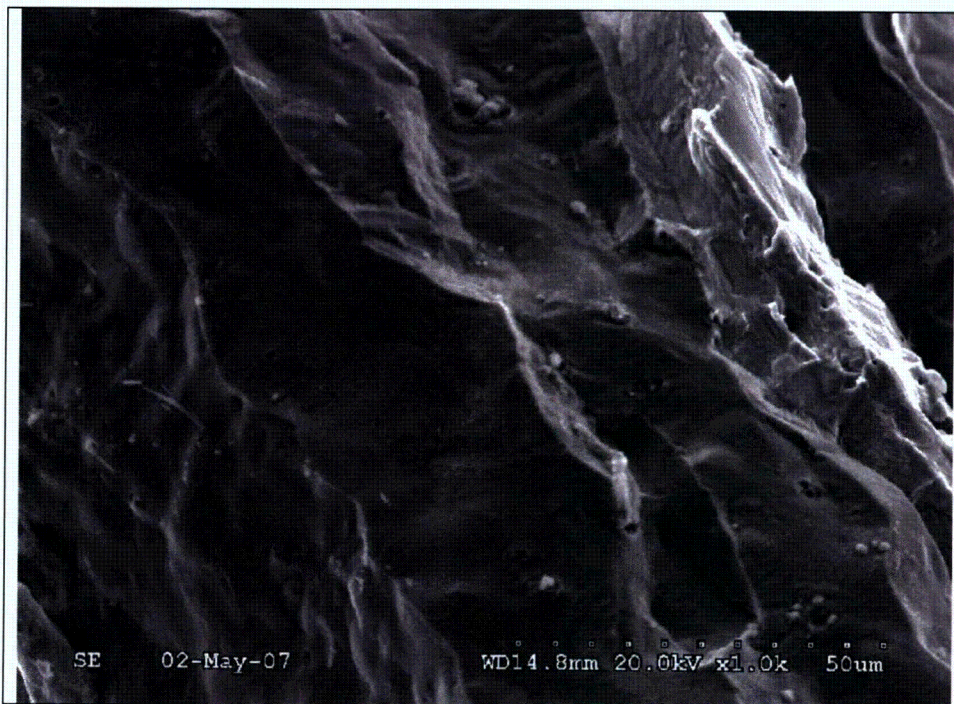


Figure 37 – An SEM photo showing a relatively smooth region of the exposed crack surface of the Sample A1 weld. (1000x Magnification)

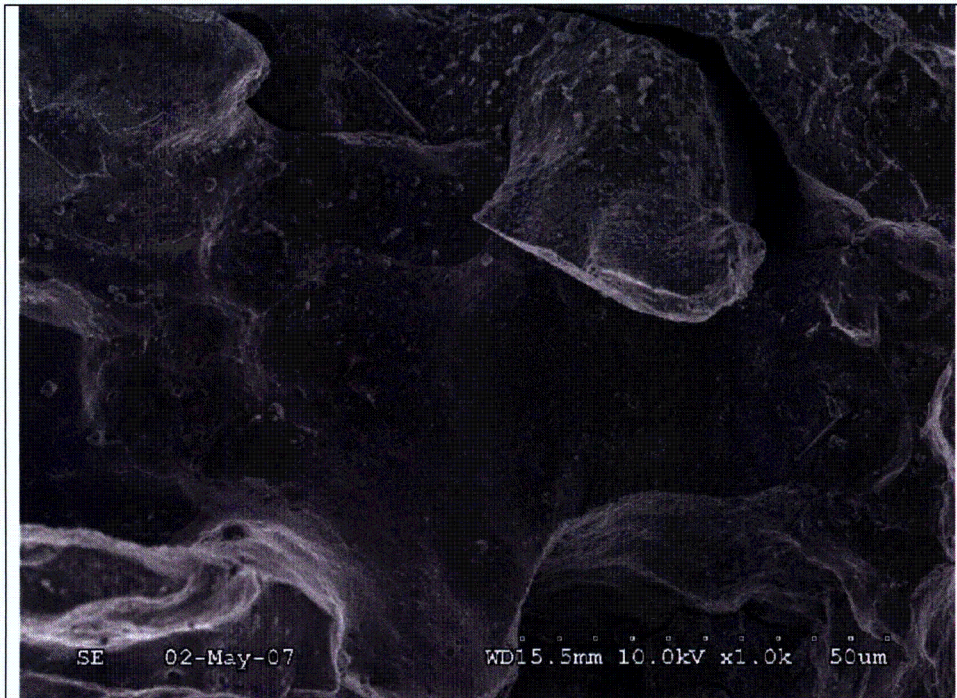


Figure 38 – Another smooth crack surface region in the Sample A1 weld. The smooth appearance is considered more typical of a hot crack than stress corrosion cracking. (1000x Magnification.)

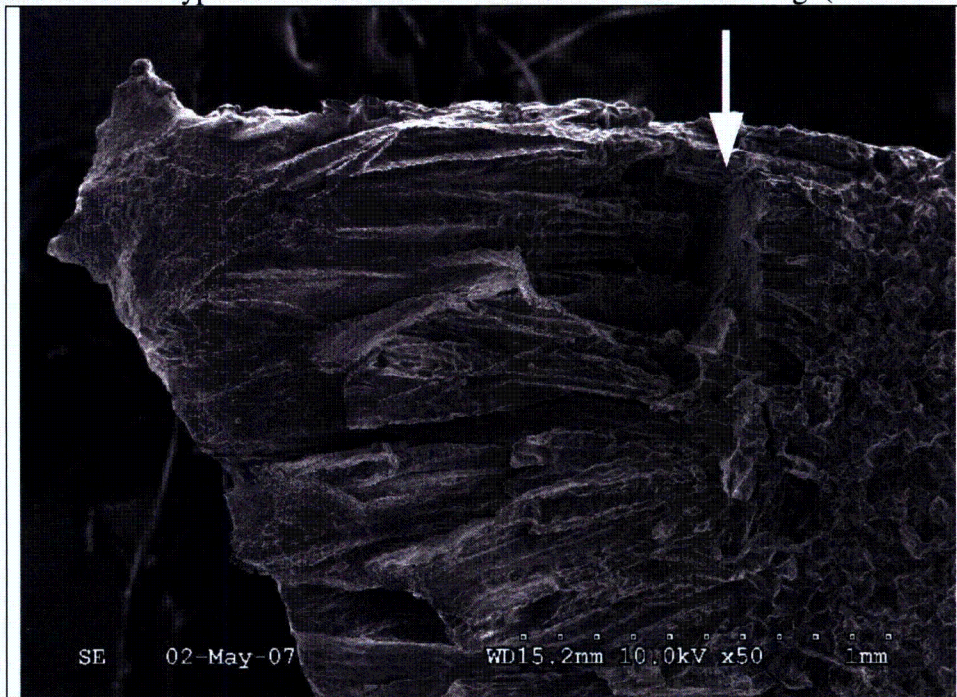


Figure 39 – A SEM view of the Sample A1 crack surface near the upper end of the weld. The arrow points to a planar defect in the weld. There are several cracks within the weld that are connected to the defect. The ductile region toward the upper left corner of the sample was broken open in the lab. (50x Magnification)

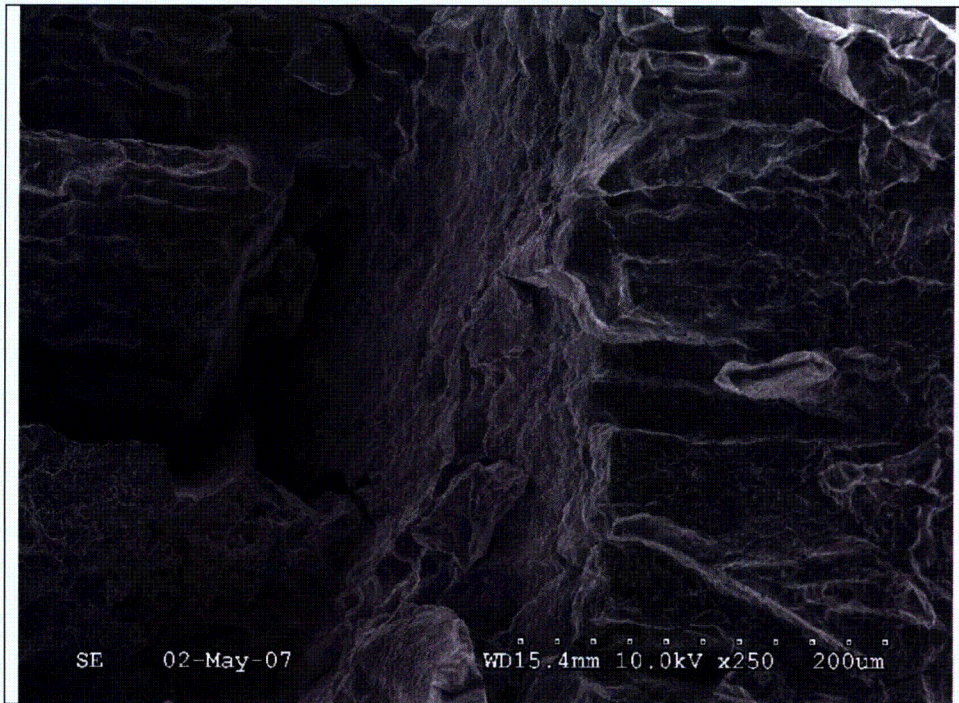


Figure 40 – A higher magnification view of the Figure 39 defect. The defect location and orientation is consistent with lack of fusion between weld passes. (250x Magnification)

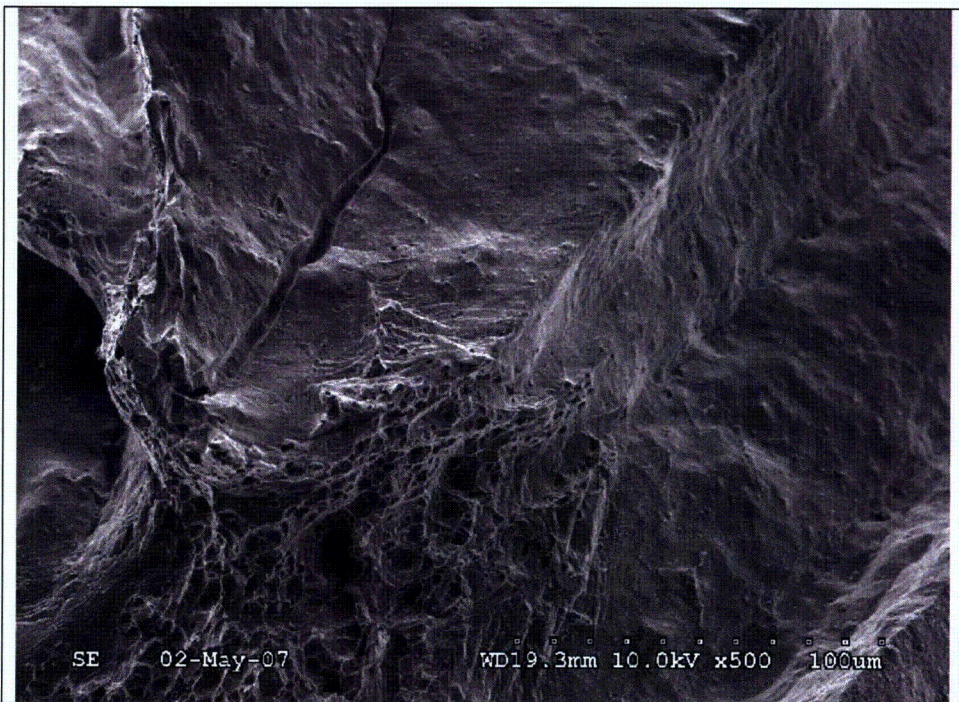


Figure 41 – A local patch of ductile dimples on the exposed crack surface in Sample A1. In general, most of the ductile patches were located toward the wetted surface of the weld. (500x Magnification)

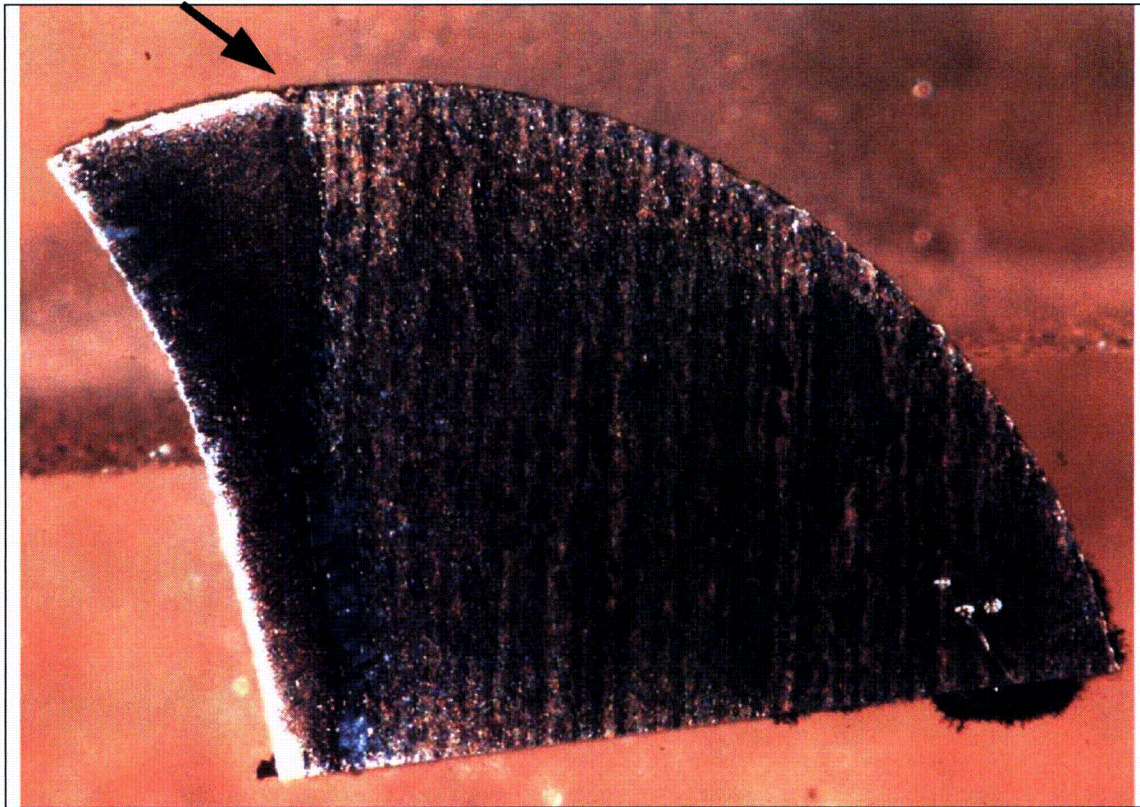


Figure 42 – A stereoscope view of metallurgical Sample A2A. The arrow points to the lack of fusion defect. (17x Magnification)

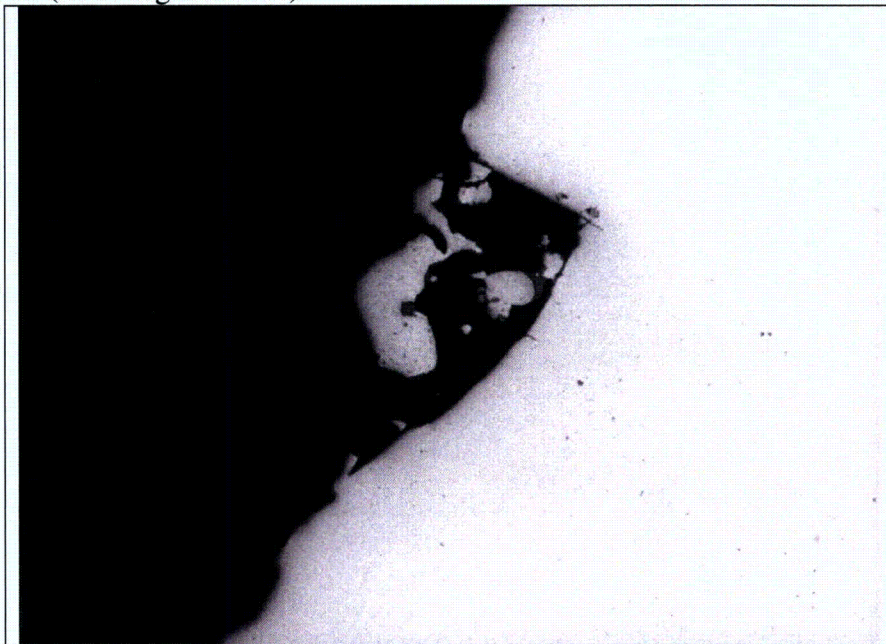


Figure 43 – An un-etched view of the lack of fusion defect. Note the globular debris from the EDM cutting process. The flat region is the tube side of the defect (190x Magnification)

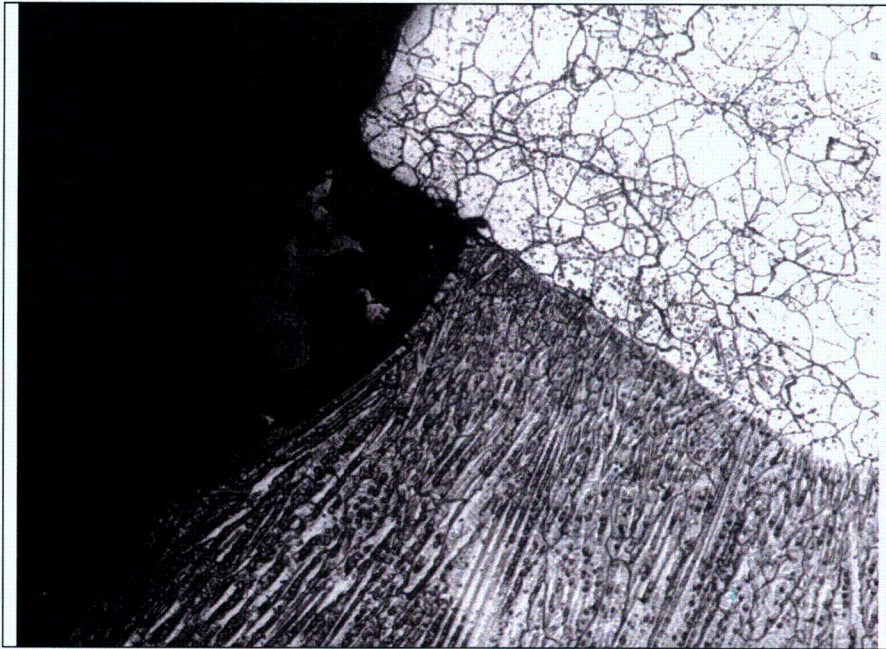


Figure 44 – An etched view of the lack of fusion defect in Sample A2A. Also note the flat interface at the fusion line, which indicates there was little penetration at this location. (190x Magnification, Electrolytic Phosphoric-Nital Dual Etch)

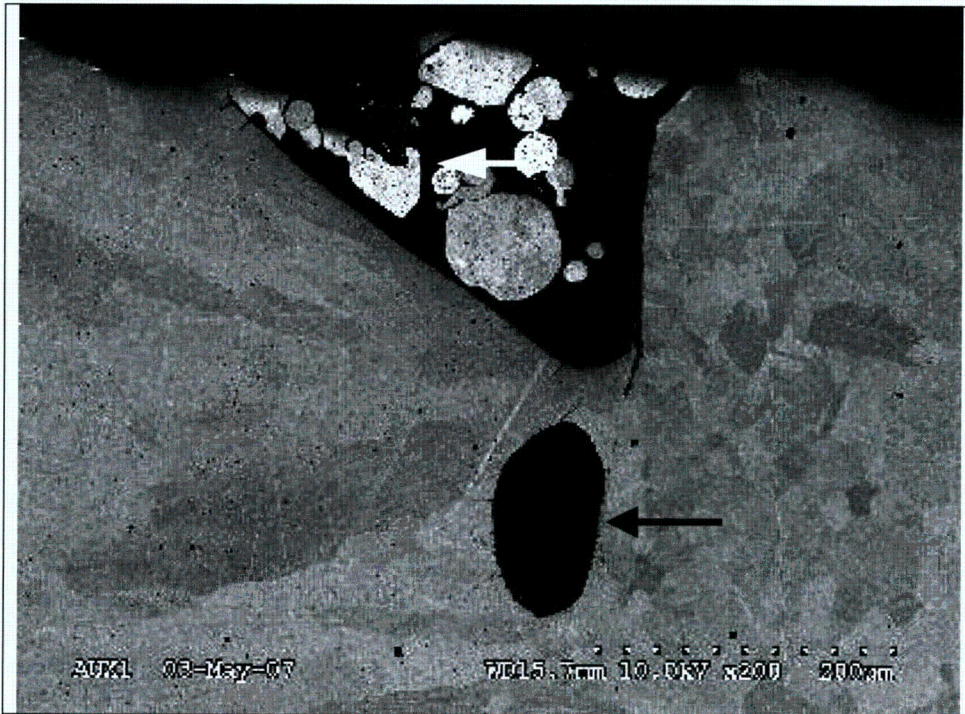


Figure 45 – A SEM photo of the Sample A2A metallurgical mount. Note the large inclusion (arrow) that is adjacent to the lack of fusion defect (200x Magnification).

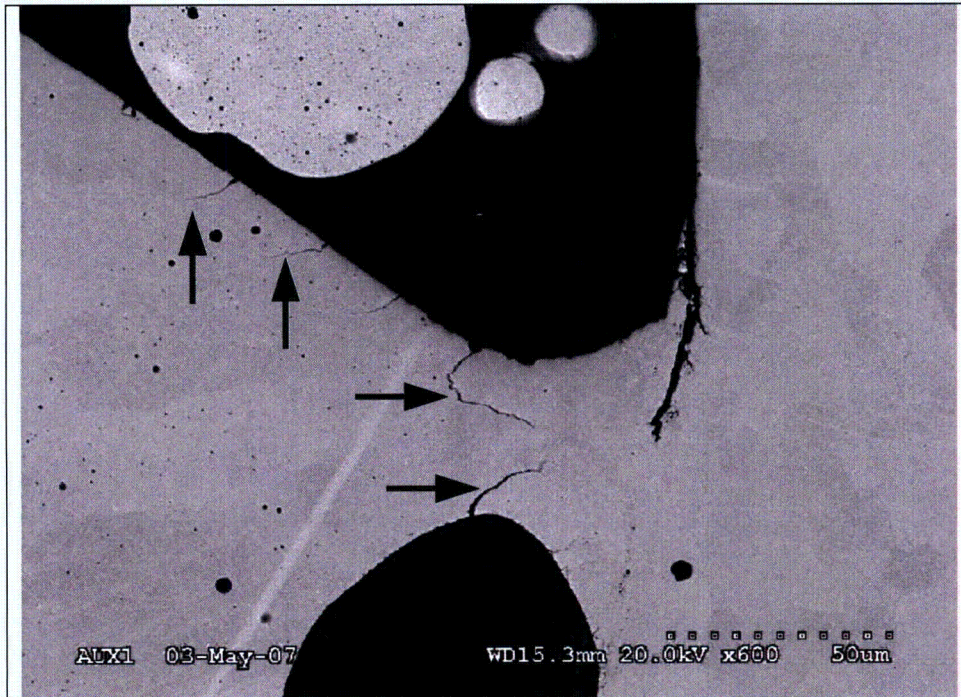


Figure 46 – A SEM photo of the Sample A2A mount. The arrows point to several incipient cracks that initiated from the inclusion and the lack of fusion defects. The defects are typical of hot cracking. (600x Magnification)

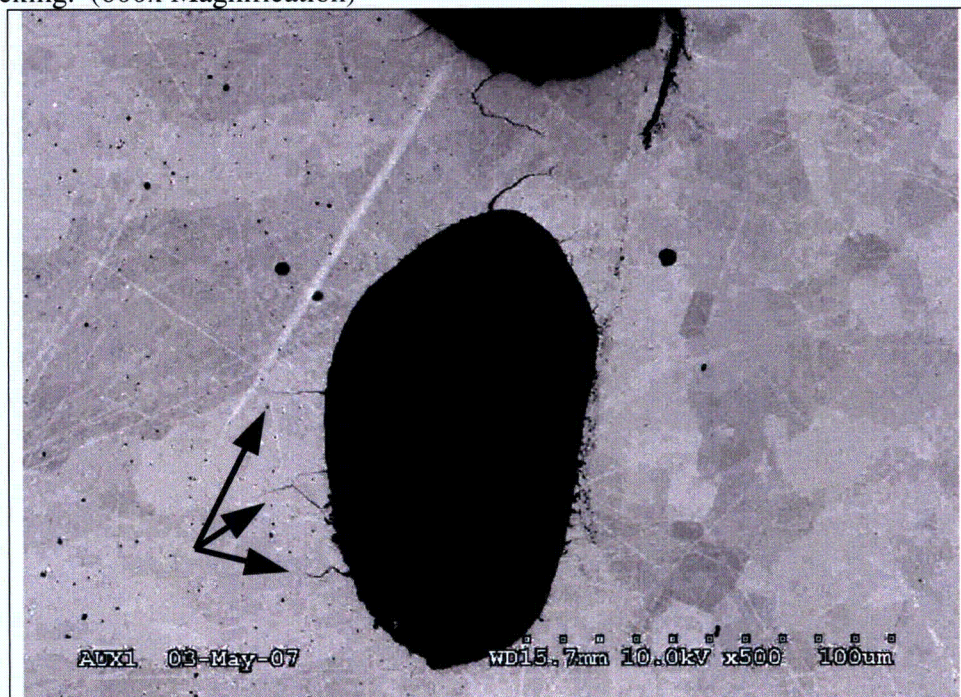


Figure 47 – Another SEM photo with arrows pointing to several cracks that initiated from the edge of the inclusion. The angled appearance of the lower two cracks appears similar to incipient PWSCC. Also note the incipient penetrations along the tube (right) side of the inclusion. (500x Magnification)

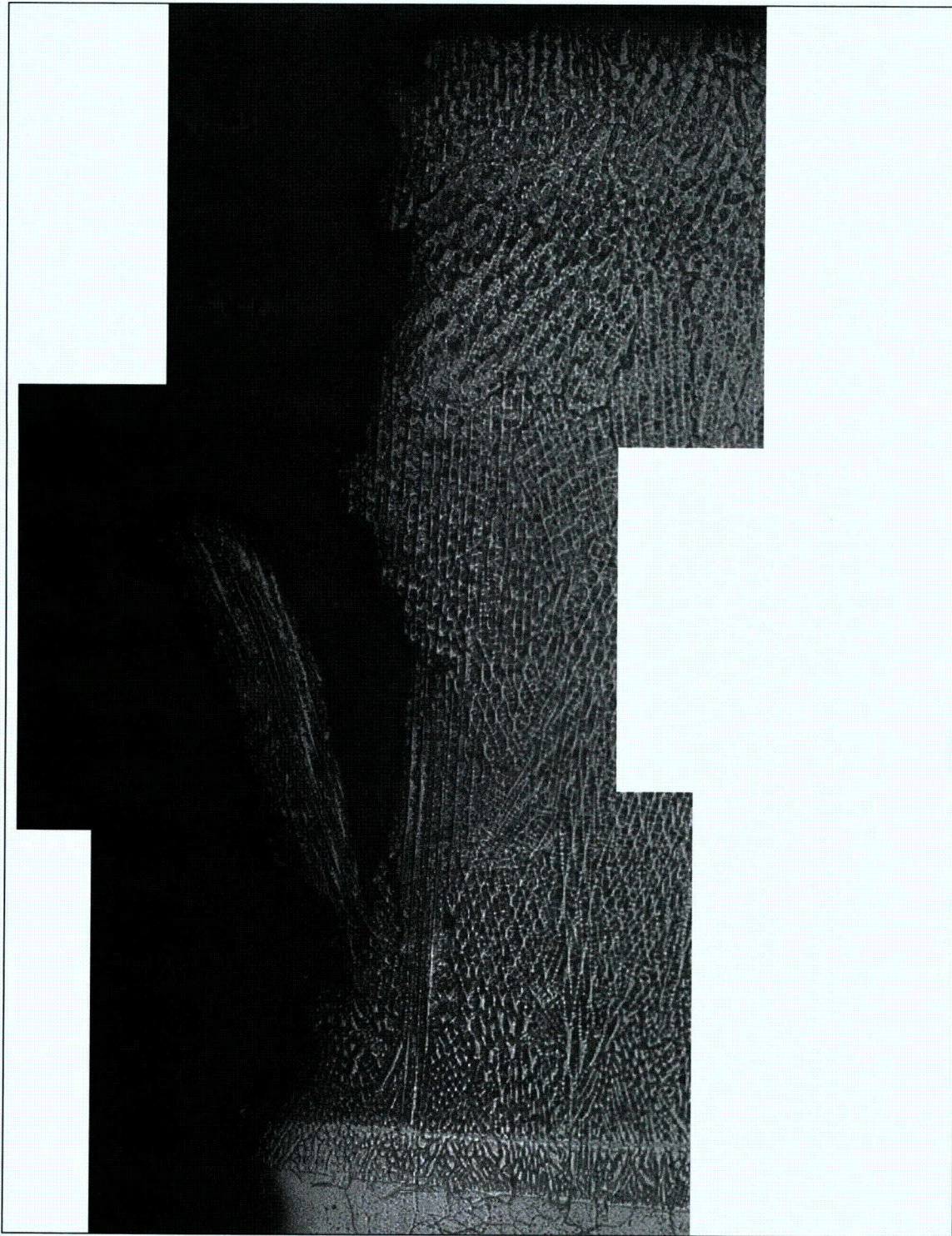


Figure 48 – A montage showing the edge of the axial crack in the Sample A2A weld. There was limited crack branching within the weld. The angled flap was likely pulled open when the crack surface was exposed in the lab. (190x Magnification)



Figure 49 – A higher magnification view of Figure 48 near the wetted surface. In this region, the only branch was angled toward the wetted surface. (375x Magnification, Electrolytic Phosphoric-Nital Etch)

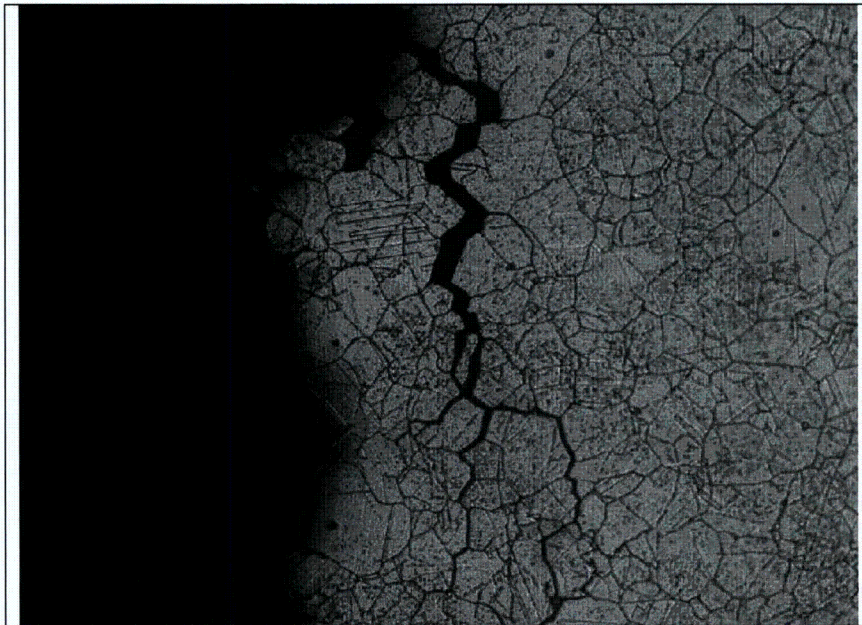


Figure 50 – An intergranular, branched crack that was connected to the axial crack in the Sample A2A tube material. (375x Magnification, Electrolytic Phosphoric-Nital Dual Etch)

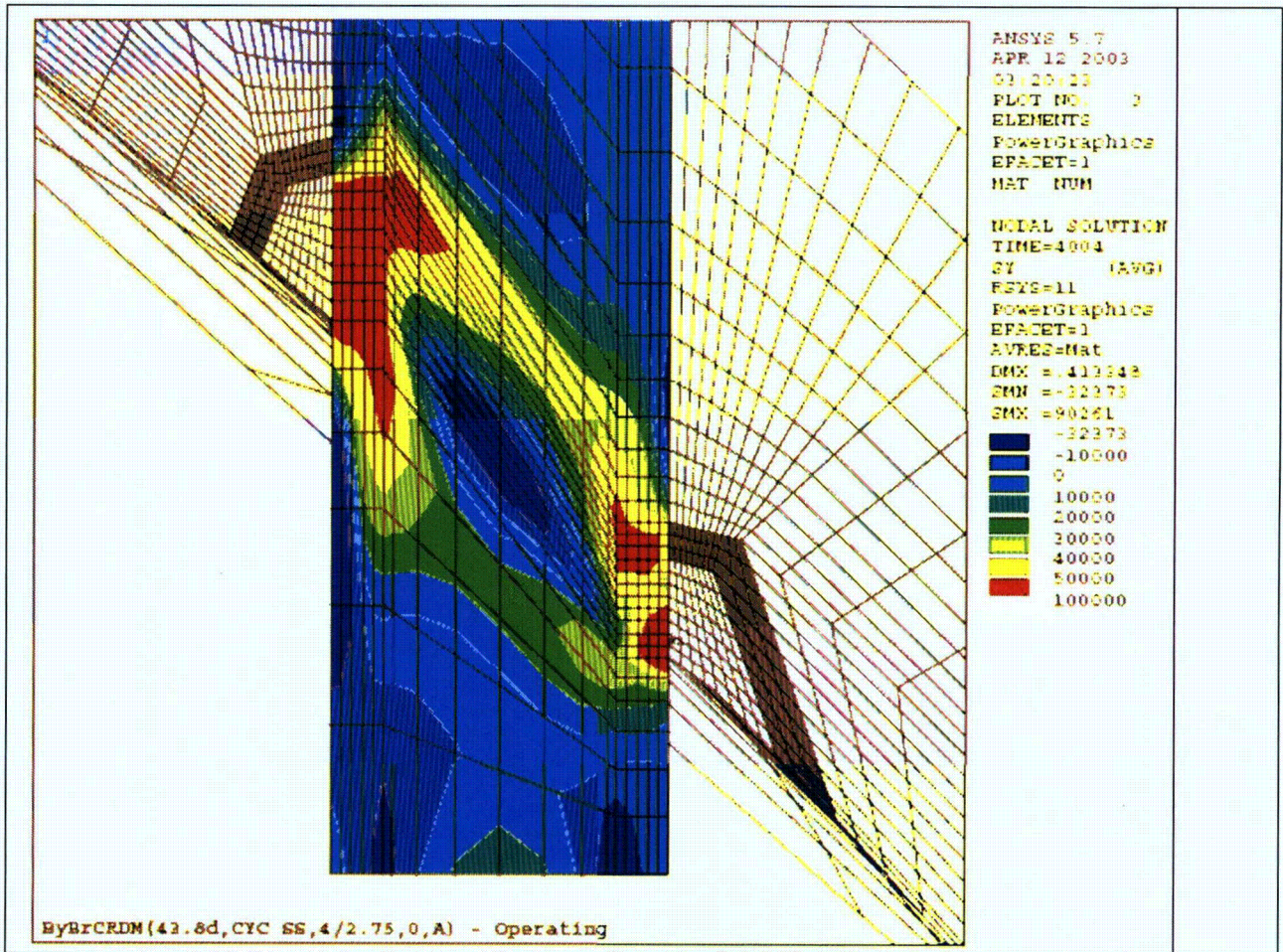


Figure 51 – A hoop stress plot from Reference 9 for the configuration that is applicable to the #68 CRDM penetration. The calculation included residual welding stresses and the stress from the operating pressure. The red areas highlight the high stress regions, which have calculated stresses between 50,000 to 100,000 psi. Note the high stress region at the downhill side of the weld corresponds to the approximate location of the axial indication in the #68 CRDM penetration.

**Laboratory Test Plan for Evaluations of a Crack Containing 'Boat' Sample  
from the #68 CRDM penetration on Byron Unit 2**

A boat sample measuring approximately 1.5" long x 0.790" wide x 0.375" deep was removed from the #68 CRDM penetration on Byron Unit 2. The sample contained a portion of the UT and dye penetrant indications that were detected during Byron B2R13 outage inspections. Photos of the field dye penetrant results for the original indications and the boat sample excavation site are shown in Figures 1 and 2. The removed boat sample is shown in Figures 3 and 4. This document identifies the laboratory test plan developed for the indications in the removed boat sample. (Note: This test plan has been slightly modified from the 'Preliminary' test plan due to the smaller dimensions of the removed boat sample.)

(Note: The relevant results for each test plan step shall be documented by photographs.)

1. Perform low magnification visual and stereoscope inspections (up to 50x) of the external surfaces of the boat sample. Look for surface connected indications, anomalies and other distinguishing features that may be present.
2. Perform a fluorescent dye penetrant 'Zyglo' examination of the boat sample surfaces to determine the location of surface connected indications. Prior to performing the Zyglo exam, the sample will be ultrasonically cleaned in an iso-propanol bath to remove the remnants of the red dye penetrant exams that were performed in the field. The field NDE results from the boat sample excavation site should also be reviewed for potential crack locations.
3. Perform a scanning electron microscope (SEM) examination of the cut and non-cut surfaces of the of the boat sample. The sample will need to be re-cleaned by ultrasonic techniques prior to SEM exam. The purpose is to characterize any defects on the surface and to look for tight defects/cracking that may not have been detected by the Zyglo examination. These results should be compared to the field dye penetrant results for the boat sample excavation site.
4. Perform X-ray radiography exams at several orientations/angles to characterize flaws locations within the boat sample.
5. (Exelon Review Hold Point) Depending on the results of steps 1 thru 4, a sectioning plan will be developed to characterize microstructure, crack depth and crack morphology. The goal of the sectioning plan is to allow for completion of steps 6 thru 10. The sample sectioning should be performed with a diamond (or other thin) cutting wheel to minimize material loss. The on-site Exelon representative (or other Exelon designee) can remove the hold point. As the sectioning cuts are performed, the cut faces should be examined at low magnification for cracking and/or other defects.
6. Prepare a metallurgical mount through a portion of the surface connected linear indication. The mount orientation should be approximately perpendicular to the linear indication. The primary goals of the mount are to characterize the mode of crack propagation, evaluate the weld microstructure, and look for weld defects and other anomalies. If large inclusions or other anomalies are identified, they should be evaluated by SEM/EDS techniques. Prior to

performing metallurgical etching, the lab technician shall demonstrate the suitability of the etchant and etching procedure on a sample with a similar material chemistry. If necessary, multiple grind-polish-examine sequences can be performed to evaluate specific microstructure features. If multiple grinding sequences are performed, the amount of removed material should be measured and recorded.

7. Expose a portion of the linear indication that was detected by the field dye penetrant examination. Examine the exposed surface by scanning electron microscopy and semi-quantitative EDS techniques. The goals of this step are to characterize the crack surface features, identify an initiating region (if present), look for defects/anomalies, and characterize the composition of the oxidation/corrosion products of the crack surface. If there is heavy oxidation on the exposed crack surface, it may be necessary to clean the surface (after the EDS evaluations are completed).
8. It is anticipated that at least three additional metallurgical mounts will be prepared. The specific location and goals for the additional mounts will not be determined until the results from the previous steps have been evaluated. It is expected that one of the mounts will evaluate the indication that corresponds to the dye penetrant indication in the boat sample excavation.
9. Chemical Analysis: If sufficient material exists, a full chemical analysis will be performed on the tube and weld metal to allow for comparison to fabrication specifications. The facility should ensure that appropriate reference standards are available for the chemical analysis technique (e.g., ICP techniques). If the sample size is too small for a full chemistry, semi-quantitative EDS evaluations of the weld and base metals shall be performed on the metallurgical samples. EDS evaluations shall also be performed on any microstructural anomalies that were identified in the metallurgical mounts (e.g., large inclusions).
10. Perform Knoop micro-hardness traverses on areas of interest in the metallurgical mounts.

**Additional Requirements:**

- The lab facility shall allow for both Exelon and the NRC personnel to witness the lab evaluations.
- The lab facility shall be prepared to store the sample remnants for at least 1 year. The facility shall not dispose of the sample remnants without Exelon approval.

The initial laboratory report will cover the work that is identified in steps 1 thru 10. Depending on the lab results, additional materials characterization by advanced microscopy techniques could be considered (e.g., ATEM, TEM, X-ray diffraction).

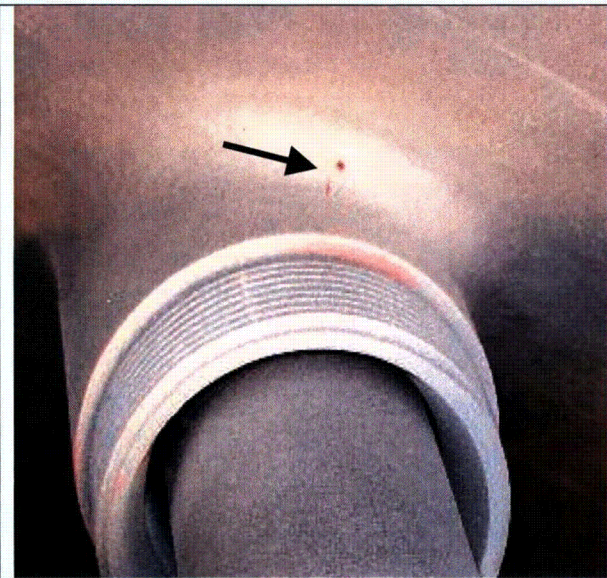


Figure 1 – A photo showing the original linear and rounded dye penetrant indications.



Figure 2 – A photo showing the dye penetrant indications at the boat sample excavation site.



Figures 3 and 4 – Photos showing the upper and lower sides of the removed boat sample.